International Journal of Biological Macromolecules 219 (2022) 224–245

Contents lists available at ScienceDirect

International Journal of Biological Macromolecules

journal homepage: www.elsevier.com/locate/ijbiomac

Biological activities and physicochemical characterization of alkaline lignins obtained from branches and leaves of *Buchenavia viridiflora* with potential pharmaceutical and biomedical applications

Denise Maria Figueiredo Araújo [a], Iranildo José da Cruz Filho [b], Tiago Santos [a], Daniel Tarciso Martins Pereira [c], Diego Santa Clara Marques [b], Alice da Conceição Alves de Lima [b], Thiago Mendonça de Aquino [d], George Jackson de Moraes Rocha [e], Maria do Carmo Alves de Lima [b,*], Fátima Nogueira [a]

[a] Global Health and Tropical Medicine, GHTM, Institute of Hygiene and Tropical Medicine, IHMT, Universidade Nova de Lisboa, 1349-008 Lisbon, Portugal
[b] Federal University of Pernambuco, Department of Antibiotics, Biosciences Center, 50.670-420 Recife, PE, Brazil
[c] Federal University of Amazonas, Institute of Exact Sciences and Technology, 69103-128 Itacoatiara, AM, Brazil
[d] Federal University of Alagoas, Institute of Chemistry and Biotechnology, 57072970 Maceió, AL, Brazil
[e] Brazilian Biorenewables National Laboratory (LNBR), Brazilian Center for Research in Energy and Materials (CNPEM), Polo II de Alta Tecnologia, Rua Giuseppe Máximo Scolfaro, 10.000, PO Box 6192, 13083-100 Campinas, SP, Brazil

ARTICLE INFO

Keywords:
Lignins
Macromolecules
Amazon rainforest
Biological activities

ABSTRACT

In this work, we investigated *in vitro* different biological activities of alkaline lignins extracted from the species *Buchenavia viridiflora*, a tree from the Amazon rainforest used as a wood product. The chemical composition results for the twig and leaves were, respectively (%): cellulose (30.88 and 24. 28), hemicellulose (21.62 and 23.03), lignin (29.93 and 25.46), extractives (13.06 and 20.52), and ash (4.51 and 6.72). The yield was higher for the lignin of the branches (67.9 %) when compared to the leaves (60.2 %). Lignins are of the GSH type, low molecular weight and thermally stable. They promoted moderate to low antioxidant activity, highlighting the lignin of the branches, which presented an IC_{50} of 884.56 μg/mL for the DPPH assay and an IC_{50} of 14.08 μg/mL for ABTS. In the cytotoxicity assays, they showed low toxicity against macrophage cells (IC_{50} 28.47 and 22.58 μg/mL). In addition, they were not cytotoxic against splenocytes and erythrocytes at concentrations ranging from 100 to 6.25 μg/mL. These were able to promote splenocyte proliferation and induce the production of anti-inflammatory cytokines. And inhibit the growth of tumor cells with IC_{50} ranging from 12.63 to values >100 μg/mL and microbial at a concentration of 512 μg/mL. Finally, they showed antiparasitic activity by inhibiting the growth of chloroquine-sensitive and resistant *Plasmodium falciparum* strains. These findings reinforce that the lignins in this study are promising for potential pharmaceutical and biomedical applications.

1. Introduction

Lignin is the most abundant natural aromatic (phenolic) macromolecule present in plants [1,2]. This gives the plant strength and structural rigidity, which ensure the transport of water and nutrients, and protection against the action of pathogens, preventing degradation [1–3]. Lignin is amorphous, dense, and complex, its chemical structure consists of three different phenylpropane units: guaiacyl (G), syringyl (S), and *p*-hydroxyphenyl (H), respectively [3,4]. These units are linked by different bonds, it is estimated that there are >10 different chemical bonds between the CO and CC atoms that form the lignin molecule, of which the main bonds present in native lignin are: β-O-4, β-β, β-5, 5-5 and 4-O-5 [1–3].

The biosynthesis of these macromolecules begins in the middle lamella, and this process is one of the last steps of xylem cell differentiation [5–7]. The lignin-forming units are the p-coumaryl, coniferyl phenylpropanoids, and synapyl alcohol [3,6,7]. The formation of these monolignols occurs with the reduction of the respective acid groups by the nicotinamide adenine dinucleotide phosphate (NADPH) molecule [1–3]. The macromolecular structure is synthesized in plants through a

* Corresponding author.
E-mail address: maria.calima@ufpe.br (M. do Carmo Alves de Lima).

https://doi.org/10.1016/j.ijbiomac.2022.07.225
Received 29 June 2022; Received in revised form 22 July 2022; Accepted 28 July 2022
Available online 1 August 2022

mechanism of dehydrogenative (enzyme-mediated) polymerization of monolignols, giving rise to the G, S, and H units of lignin [2,3]. Units link together randomly favoring different chemical structures [1,2]. Traditionally, lignins are obtained as a co-product of the pulp and paper industry and are burned in boilers to obtain energy [8,9].

However, several studies have been carried out to obtain products with high added value using lignin as a raw material. These macromolecules have various applications and can be used as a binding agent [10], fuel [11], carbon fibers and renewable materials [12], fertilizers [13], films [14], sunscreens [15], in addition, it can be used as raw material more sustainable for the construction industry [16] and use of lignin in the field of energy capture as a dopant for carbon-based semiconductors [17,18].

Regarding biological activities, these may have antioxidant [15,19,20], lignin-based nanomaterials for early glucose detection [21], immunological [19,22], antimicrobial [23], antitumor [24], antiparasitic [20]. In addition to these applications, they can be used as vehicles for controlled drug delivery [25–29].

All these applications are directly conditioned to the phenolic structure of these lignins. The chemical structure may vary according to the extraction method, procurement and source [30–33]. In addition, these can be fractionated or modified in order to have a greater increase in biological activity [30,33].

In this sense, the search for 'new' lignins is necessary and several plants have been studied, among the different species, we highlight the species *Buchenavia viridiflora*. Popularly known as "Taniboca" is a tree found in the Brazilian Amazon Forest for commercial use as a timber species. Due to a very scarce knowledge about the biological applications of its constituents, we chose to study the lignins of this plant and evaluate its cytotoxic, immunomodulatory, antitumor, antimicrobial, and antiparasitic potential *in vitro*.

In this context, the present work aimed to obtain two lignins extracted from branches and leaves of *Buchenavia viridiflora*, a plant of great commercial interest for the timber sector. This study brings as a novelty the pioneering application of these lignins in different *in vitro* biological assays. All these tests were carried out to use these macromolecules as raw material to obtain products with high aggregate to be used in the pharmaceutical and biomedical areas.

2. Materials and methods

2.1. Reagents

ABTS (Merk, CAS 28752-68-3), acetone (Merk, CAS 67-64-1), acetonitrile (Merk, CAS 75-05-8), Acetic Acid (Merk, CAS: 64-19-7), Ascorbic acid (Cewin), phosphoric acid (Merk, CAS 7664-38-2), gallic acid (Meta Química, CAS 149-91-7), sulfuric acid (Merk, CAS 7664-93-9), albumin (Merk, CAS 9048-46-8), carbonic anhydrase (Sigma-Aldrich, CAS 9001-03-0), acetic anhydride (Merk,CAS:108-24-7), aprotinin (Sigma-Aldrich, CAS 9087-70-1), arabinose (Merk, CAS 5328-37-0), cellobiose (Merk, CAS 528-50-7), cyclohexane (Merk, CAS 110-82-7), cytochrome *c* (Merk), lead citrate (Chem Xinglu Chemical, CAS 512-26-5), calcium chloride (Merk, CAS 10043-52-4), dimethylsulfoxide (Merk, CAS 67-68-5), deuterated dimethyl sulfoxide (Merk, CAS: 2206-27-1), DPPH (Merk, CAS 1898-66-4), ethanol (Merk, CAS 64-17-5), potassium ferricyanide (Merk, CAS 13746-66-2), furfural (Merk, CAS 98-01-1), glucose (Merk, CAS 50-99-7), , sodium hydroxide (Merk, CAS1310-73-2), hydroxymethylfurfural (Merk, CAS 67-47-0), sugarcane bagasse lignin (Laboratory of Biotechnological Processes, UFPE), methanol (Merk, CAS 67-56-1), ammonium molybdate (Sigma-Aldrich, CAS 12054-85-2), potassium persulfate (Dynamics Formula), pyridine (Merk,CAS: 110-86-1), xylose (Merk, CAS 58-86-6), RPMI 1640 culture medium (Thermo Fisher Scientific), triton-X (Merk, CAS 9036-19-5), green fluorescent protein (BioLinker), chloroquine (Merk, CAS: 50-63-5), MTT Formazan (Merk, CAS:57360-69-7), SYBR green I (Invitrogen, Thermo Fisher Scientific).

2.2. Material plant

The branches and leaves of the species *Buchenavia viridiflora* were kindly provided by the company Mil Madeiras Preciosas Ltda (PRECIOUS WOODS) http://preciouswoods.com.br/ located in the municipality of Itacoatiara in the State of Amazonas, Brazil. This company carries out sustainable forest management operations, standing out as a reference in the field of wood products from native forests in Brazil and the world. The species was registered in SisGen (National System of Genetic Heritage and Associated Traditional Knowledge), no A36E658.

Initially, the branches and leaves (separately) were dried at 60 °C for 48 h in an oven (Tecnal, TE-393/1), then they were ground in a knife mill (Fritsch – Pulverisette 14) and sieved to granulation of 80 mesh. Finally, they were stored at 30 °C.

2.3. Analysis of the chemical composition of branches and leaves

The analysis of the composition of branches and leaves was carried out using the adapted methodology of Silva et al. [20]. Initially, the ground plant material (80 mesh) was subjected to extraction in a Soxhlet apparatus, until the extracting solvent (cyclohexane/ethanol; 50:50 *v*/v) became colorless (removal of extractives).

The solid obtained was dried in an oven at 105 °C until constant weight (this procedure allows for determining the percentage content of extractives present in the plant material). Then, the extractive-free material (2 g) was transferred to a 100 mL beaker with 15 mL of 72 % (*v*/v) sulfuric acid. The mixture was continuously stirred in a thermostatic bath at 45 °C for 12 min. The reaction was stopped by adding a volume of 275 mL of distilled water and this system (solid + acid hydrolyzate) was transferred to an Erlenmeyer flask and autoclaved at 121 °C for 30 min. At the end of autoclaving, the system was cooled and the suspension was transferred to a 500 mL flask. The volume was made up of distilled water, homogenized, and filtered. The solid residue (insoluble lignin + ash), after several washings, was dried in an oven at 105 °C until constant weight. Through the difference between the residue mass and the ash mass, the percentage of insoluble lignin was determined.

The liquid fraction was analyzed by high performance liquid chromatography to determine glucose, xylose, arabinose, furfural and hydroxymethylfurfural, to calculate the percentage of cellulose, hemicellulose and soluble lignin.

To determine the total ash content, 1 g of the material (*in natura* branches or leaves) was heated in a muffle furnace at 800 °C for 4 h. After cooling, the calcined material was weighed and the ash content was determined by mass difference. All experiments were performed in triplicate.

2.4. Process of extraction and obtaining of lignin

The lignin was obtained according to the methodology used by Cruz-Filho et al. [22], Santos et al. [19], Melo et al. [23], Arruda et al. [15], and Silva et al. [20] with few modifications. Initially, 100 g of branches or leaves of *Buchenavia viridiflora*, ground (80 mesh) was submitted to an aqueous extraction in a reactor in the proportions (g/L) 1:1, in a 2 L reactor, at 60 °C and 1200 rpm, for 1 h. The solid material obtained was submitted to an acid pre-treatment in an autoclave under the following conditions: proportion: 1:1 solid: liquid (g/L), H_3PO_4 (1 %) at 121 °C for 1 h. The liquid was separated from the resulting solid by filtration. Then the resulting solid was subjected to alkaline delignification using 1 % NaOH. The conditions were the same as in the acid pretreatment. After completion of the reaction, the black liquor was separated from the resulting solid by filtration, and H_2SO_4 was acidified to pH 2 for 12 h to obtain lignin (precipitation). Then the solid was filtered and dried at 70 °C for 48 h.

The yield obtained for the two lignins (one from the branch and the other from the leaf) was calculated using Eq. 1 proposed by Guo et al.

[34], Gilarranz et al. [35], and Arruda et al. [15] and Silva et al. [20].

$$Y(\%) = \left(\frac{\text{Mass of lignin extracted}}{\text{Total lignin mass in branches or leaves}}\right) * 100\% \quad (1)$$

2.5. Physical and chemical characterization of the lignins obtained

2.5.1. Elementary analysis

The contents of carbon, hydrogen, nitrogen, and oxygen (by estimate) present in the lignin structures were determined by elemental analysis [36]. This technique is characterized by the dynamic combustion of a certain amount of lignin which is introduced into the combustion reactor [15,36–38]. The assays were performed using 2 mg lignins and these were analyzed in triplicate on a Perkin-Elmer brand elemental analyzer, model 2400 Series II CHNS/O.

2.5.2. Fourier transform attenuated total reflection spectroscopy (ATR-FTIR)

The functional groups present in the lignin structures were determined by ATR-FTIR [15,20,23]. Approximately 100 mg of lignin were pressed to form a 12 mm diameter and 1 mm thick disc. The spectra were obtained in triplicate on a Perkin Elmer spectrophotometer (FT-IR Spectrum Two – UART Two) in the region from 600 to 4000 cm^{-1}.

2.5.3. Ultraviolet visible spectroscopy (UV/Vis)

UV/Vis analysis gives us information about the aromatic nature of lignins [39,40]. The experiments were carried out according to methodologies proposed by Melo et al. [23], Arruda et al. [15], and Silva et al. [20] with few modifications. Initially, the lignins were solubilized in 0.01 mol/L sodium hydroxide (pH = 12) at a concentration of 0.5 g/L. Then, the maximum absorption lengths of the lignin solutions were determined, and analyzed in a Hewlett-Packard spectrophotometer, model 8453, at wavelengths ranging from 190 to 700 nm. Sodium hydroxide solution (0.01 mol/L) was used as a blank for the equipment. In addition to the maximum wavelength, the molar absorptivity coefficient was determined at a wavelength of 280 nm. For this, solutions of different concentrations of lignin (concentrations 0.001 to 0.5 g/L) were prepared in sodium hydroxide 0.01 mol/L. Then, the absorbances referring to each one of the concentrations were determined in a Hewlett-Packard spectrophotometer, model 8453. The sodium hydroxide solution was used as the equipment blank. The results were analyzed by linear regression between the concentration and the determined absorbance. The experiments were carried out in triplicate.

2.5.4. Acetylation of lignin and characterization by nuclear magnetic resonance

Acetylation was performed according to the procedure described by Cruz-Filho et al. [22], Santos et al. [19], Melo et al. [23], and Arruda et al. [15], and Silva et al. [20] with few modifications. About 30 mg of lignin were dissolved in 5 ml of pyridine and 5 mL of acetic anhydride. The mixture was bubbled for 15 min with nitrogen and the vial was sealed. The system was left at room temperature in the dark for 50 h. At the end of the reaction, excess acetic anhydride was removed by adding 4 mL of methanol. The solvents were evaporated under reduced pressure, with the aid of azeotrope formation with toluene and ethanol. Finally, the samples were completely dried for three days under a vacuum. The acetylation process was carried out to increase the solubility of lignin in organic solvents.

Acetylated lignins (20 mg) were dissolved in deuterated DMSO (DMSOd6) and analyzed in a BRUKER Avance 400 MHz spectrometer. (RMN-^{1}H: 400 MHz, NMR—^{13}C: 100 MHz) with Fourier transform, chemical shifts were expressed in δ (ppm) and coupling constants (J) described in Hertz (Hz) at a temperature of 20 °C. The spectra obtained were ^{1}H NMR, ^{13}CNMR, and ^{1}H—^{13}C HSQC.

2.5.5. Thermal analysis: thermogravimetry (TG), derived thermogravimetry (DTG) and differential scanning calorimetry (DSC)

The thermal analyzes of this study were performed according to Arruda et al. [15] and Silva et al. [20]. For this, a simultaneous TG-DSC thermal analyzer, model Perkin Elmer, STA 6000, was used. The analyzes were carried out in an alumina crucible with about 10 mg of lignin in a temperature range of 30 to 650 °C under an N_2 atmosphere (flow rate of 100 mL/min) and heating rate of 10 °C/min.

2.5.6. Analytical fast pyrolysis (PY-GC/MS)

The lignin pyrolysis assays were performed according to Silva et al. [20]. Through this technique, it is possible to evaluate the presence of the different units present in the lignin. In this experiment, a fast pyrolysis analyzer coupled to GC/MS (Agilent Technologies 7890A /5975C) was used to investigate the distribution of volatiles from fast pyrolysis of lignin. For this, a 10 mg sample was added to the pyrolysis tube and the temperature was adjusted to 550 °C (the temperature that promotes the total pyrolysis of lignin), the instantaneous heating rate was 20.000 °C/s and the residence time was of 45 s. The volatiles was identified in GC/MS (model QP2010, Shimadzu), with a DB-35MS capillary column (5 m × 0.20 mm × 0.33 μm Agilent GCMS) under the conditions: helium gas with a flow of 1 mL/min, inlet temperature 300 °C, the oven temperature was programmed from 40 °C (3 min) to 200 °C (1 min) with a heating rate of 4 °C/min and then to 280 °C (1 min) with a heating rate of 20 °C/min; mass spectra were operated in electron ionization (EI) mode at 70 eV. Mass spectra were obtained from m/z 50 to 650.

2.5.7. Molecular weight determination by gel permeation chromatography (GPC)

The GPC technique was used to determine the molecular weight of the lignins under study. The experiments were carried out according to Santos et al. [19], Melo et al. [23], Arruda et al. [15], and Silva et al. [20] with few modifications. The molar mass distribution was determined using a 57 cm × 1.8 cm glass chromatographic column filled with Sephadex G-50. A 0.5 mol/L NaOH solution was used as the mobile phase at a flow rate of 0.5 mL/min. Samples were injected on top of the column (500 μL of a 1 g/L solution in 0.04 mol/L NaOH). Fractions of 4.0 mL were collected and the absorbance of each fraction at 280 nm (maximum lignin absorption wavelength) was measured in a Hewlett-Packard model 8453 spectrophotometer. The chromatography column was previously calibrated with a series of protein standards (albumin of 66,000 Da carbonic anhydrase of 29,000 Da, cytochrome C of 12,400 Da, and aprotinin of 6500 Da) and sugarcane bagasse lignin 2000 Da).

2.5.8. Determination of total phenols by the Folin-Ciocalteu colorimetric method

The quantification of the total phenolic content present in the lignins of this study was performed in triplicate, using the Folin-Ciocalteu colorimetric method (Ainsworth et al.). The experiments were carried out according to the methodology described by Cruz-Filho et al. [22], Santos et al. [19], Melo et al. [23], Arruda et al. [15], and Silva et al. [20] with few modifications. Initially, a 0.5 mL solution of lignin dissolved in 10 % DMSO at a concentration of 1000 μg/mL was added to 2.5 mL of Folin-Ciocalteu reagent diluted 1:10 and 2.0 mL of 4 % Na_2CO_3. The system was incubated in the dark for 2 h at room temperature. Subsequently, absorbance readings were performed in a Hewlett-Packard spectrophotometer, model 8453 at 740 nm. To quantify the total phenolic content, an analytical curve was constructed using gallic acid as a standard (3.9–1000 μg/mL). The result was expressed in mg of gallic acid equivalent per gram of lignin (mg GAE/g).

2.6. In vitro antioxidant activity

2.6.1. DPPH free radical scavenging activity

The antioxidant activity of the DPPH• method is based on the

principle that DPPH• (2,2-diphenyl-1-picrylhydrazine), being a stable violet-colored radical, accepts an electron or hydrogen radical to become a stable molecule, being reduced in the presence of an antioxidant and acquiring a yellow color [41,42]. As a radical, DPPH• has a characteristic absorption at 517 nm, which disappears as it is reduced by hydrogen donated by an antioxidant compound [42].

The tests were carried out according to the methodology proposed by Cruz-Filho et al. [22], Santos et al. [19], Melo et al. [23], and Arruda et al. [15] with few modifications. Initially, the lignins were diluted in 10 % DMSO at concentrations ranging from 3.9 to 1000 μg/mL. Then, aliquots of 0.5 mL of lignin were added to 3.0 mL of the DPPH radical in 0.5 mM ethanol solution and incubated for 25 min at room temperature and in the absence of light. Absorbances were determined in a Hewlett-Packard spectrophotometer, model 8453, using ethanol as the equipment blank. The standards used were ascorbic acids and butylated hydroxytoluene (BHT). The experiments were performed in triplicate. The activity kidnapping activity was determined by Eq. (2)

$$\mathrm{DPPH}(\%) = \left(\frac{A_{\mathrm{control}} - A_{\mathrm{sample}}}{A_{\mathrm{control}}}\right) * 100\% \quad (2)$$

where, $A_{control}$ is the absorbance of the control and A_{sample} is the absorbance of the sample.

Through the results obtained, it was possible to determine the IC_{50} concentration where 50 % of the DPPH radical is captured.

2.6.2. Antioxidant activity by the ABTS method

Antioxidant activity by the ABTS •+ [2,2′-azinobis-(3-ethylbenzothiazolin-6-sulfonic acid)] method is based on the energetic reaction with hydrogen donor compounds, such as phenolic compounds, being converted into a non-active compound, ABTS colored (ie, changing from green to colorless) [41,42]. The test was performed according to the methodology described by Cruz-Filho et al. [22], Santos et al. [19], Melo et al. [23], and Arruda et al. [15] with few modifications. The ABTS radical was formed by the reaction of a 7 mM ABTS •+ solution with 140 mM potassium persulfate solution, incubated at 25 °C and in the absence of light for 16 h. Once formed, the radical was diluted with ethanol P.A. until obtaining an absorbance value of 0.700 ± 0.020 at 734 nm. Initially, the lignins were diluted in 10 % DMSO at concentrations ranging from 3.9 to 1000 μg/mL. Then, a 30 μL aliquot of each lignin dilution was added to 3.0 mL of the ABTS radical. After 3 min of reaction, the absorbances were determined in a Hewlett-Packard spectrophotometer, model 8453 at 734 nm, and ethanol was used as a blank. The standards used were ascorbic acids and butylated hydroxytoluene (BHT). The experiments were performed in triplicate. The sequestration activity was determined by Eq. (3).

$$\mathrm{ABTS}(\%) = \left(\frac{A_{\mathrm{control}} - A_{\mathrm{sample}}}{A_{\mathrm{control}}}\right) * 100\% \quad (3)$$

where, Acontrol is the absorbance of the control and Asample is the absorbance of the sample.

Through the results obtained, it was possible to determine the IC_{50} concentration where there is capture of 50 % of the ABTS radical.

2.6.3. Evaluation of antioxidant activity by the phosphomolybdenum complexation method

This method is based on the reduction of molybdenum (VI) to molybdenum (V), this reduction occurs in the presence of certain substances with antioxidant capacity, resulting in the formation of a green complex between phosphate/molybdenum (V), at acidic pH, which is determined by spectrophotometry at 695 nm [43,44]. The phosphomolybdenum complex is formed by the reaction of a solution of sodium phosphate (0.1 mol/L) with a solution of ammonium molybdate (0.03 mol/L) and a solution of sulfuric acid (3 mol/L) in an aqueous medium [43,44].

The tests were carried out according to Santos et al. [19], Melo et al. [23], and Arruda et al. [15] with few modifications. In this methodology, the phosphomolybdenum complex (3 mL) and distilled water (6.9 mL) were added to aliquots of the lignins diluted in DMSO (10 %) at concentrations ranging from 3.9 to 1000 μg/mL. The blank was obtained using 3 mL of reagent and 7.0 mL of distilled water. All tubes were incubated at 95 °C for 90 min, after cooling, the reading was taken at 695 nm, in Hewlett-Packard, model 8453. The standards used were ascorbic acids and butylated hydroxytoluene (BHT). All analyzes were performed in triplicate. The kidnapping activity was determined by Eq. (4).

$$\mathrm{TAA}(\%) = \left(\frac{\mathrm{Abs\ sample} - \mathrm{Abs\ blank}}{\mathrm{Abs\ standard} - \mathrm{Abs\ blank}}\right) * 100\% \quad (4)$$

where: Abs sample: sample absorbance. Abs blank: blank absorbance. Abs standard: pattern absorbance.

The antioxidant potential was measured by the effective concentration to reduce 50 % of molybdenum ions present in the medium (IC_{50}).

2.6.4. Assessment of reducing power

The main objective of this colorimetric method is to detect by spectrophotometry the presence of reducing groups due to their ability to reduce ferric iron (Fe^{3+}), present in the ferrocyanide complex, to ferrous iron (Fe^{2+}). The tests were carried out according to the methodology proposed by Barapatre et al. [45] with few modifications. Initially, the lignins were diluted in 10 % DMSO at concentrations ranging from 3.9 to 1000 μg/mL. Then, 0.5 mL aliquots were added to 2.5 mL of 1 % potassium ferrocyanide solution. The mixture was incubated in an oven at 50 °C for 20 min. Next, 2.5 mL of a 10 % trichloroacetic acid solution were added and the mixture was centrifuged at 3000 rpm for 8 min. After centrifugation, a 2.5 mL aliquot of the upper layer of the mixture was transferred to a test tube and 2.5 mL of distilled water and 0.5 mL of 0.1 % ferric chloride were added. The spectrophotometric readings were performed at 700 nm in a Hewlett-Packard spectrophotometer, model 8453. The blank of the samples consisted of 1 mL of water and all other reagents. The standards used were ascorbic acids and butylated hydroxytoluene (BHT). The antioxidant potential was measured by the effective concentration to reduce 50 % of iron ions present in the medium (IC_{50}).

2.7. Cytotoxicity assays in animal cells and in vitro

2.7.1. Cytotoxicity assays in J774 A.1 macrophage cells

Cytotoxicity analyzes were performed using the MTT technique, described by Silva et al. [20] with slight modifications. For this essay, the effect of lignins against J774 A.1 macrophage cells was evaluated. For this, cells were seeded in 96-well plates containing RPMI medium with phenol red supplemented with 10 % FBS and 1 % antibiotic, at a concentration of 1×10^6 cell/well and incubated in an atmosphere at 5 % CO_2 and 37 °C After 24 h, the medium was removed and the cells were incubated in the presence of different concentrations (6.25 to 100 μg/mL) of lignins for 72 h. After this period, 10 μL of MTT (5 mg/mL) was added and incubated for 3 h in an oven at 37 °C and 5 % CO_2. Then, formazan crystals were solubilized in dimethyl fulsoxide (DMSO) and their absorbance was determined by spectrophotometry at 540 nm. Wells containing RPMI and MTT medium were used as reaction controls. Each test was performed in biological triplicate and technical quadruplicate. Cell viability results were determined by Eq. (5).

$$\text{Cell viability } (\%) = \left(\frac{\mathrm{VC}}{\mathrm{TC}}\right) * 100\% \quad (5)$$

where: VC is the number of viable cells at different concentrations of lignin, TC is the concentration of viable cells in the control (only cells and culture medium) which represents 100 % viability.

The results were expressed by graphs of concentration x cell viability and by the cytotoxic concentration of lignin that inhibits 50 % of the

viability of J774 A.1 macrophage cells (IC_{50} μg/mL), obtained from non-linear regression. In addition to cytotoxicity, the production of nitric oxide in macrophage culture supernatants was determined using the Griess colorimetric method. The absorbance readings were taken in a spectrophotometer (Bio-Rad 3550, Hercules, CA) at 595 nm.

2.7.2. In vitro hemolytic activity

In vitro hemolysis assays aim to evaluate the toxicity of different compounds, whether natural or synthetic, against erythrocytes [46,47]. Initially, stock solutions at a concentration of 100 μg/mL (containing the twig and leaf lignins) were prepared in 100 % dimethyl sulfoxide (DMSO) and sterilized by filtration on a 0.22 μm filter. Then the solutions were serially diluted 1:3 at concentrations ranging from 0.02 to 50 μg/mL in a complete culture medium (RPMIc).

The evaluation of hemolytic activity was performed by incubating healthy 0Rh + erythrocytes in different concentrations of lignin. Briefly, a 3 % HTC hematocrit suspension of uninfected red blood cells (RBCs) in RPMIc was cultured for 72 h under standard culture conditions (37 °C, 5 % CO_2, and 90 % N_2) in different concentrations of lignins. A 20 % Triton™-X solution was used as a positive control (promotes 100 % hemolysis) and the negative control consisted of cell suspension only. As standard drugs, chloroquine and dihydroartemisinin were used under the same experimental conditions as the lignins in this study.

After the incubation period, the cells were centrifuged at 2000 rpm/5 min and the supernatant was used to assess hemolytic activity by quantifying the release of hemoglobin, *via* spectrophotometric absorbance measurement at 450 nm with a multimode microplate reader (Tríad, Dynex Technologies). The average percentage of hemolysis was calculated from at least two independent experiments, each in triplicate, using Microsoft Excel software through Eq. (6). Where the average absorbance of the negative control was subtracted from the sample and the average absorbance of the positive control to remove background absorbance readings:

$$\%\text{Hemolysis} = \frac{(\text{Sample absorbance} - \overline{X}\,\text{Negative Control absorbance})}{(\overline{X}\,\text{Positive Control absorbance} - \overline{X}\,\text{Negative Control absorbance})} \times 100 \quad (6)$$

In general, any compound below 10 % hemolysis is non-hemolytic, while values above 25 % hemolysis are classified as hemolytic. This study was approved by the Animal Use Ethics Committee of Institute Aggeu Magalhães/Oswaldo Cruz Foundation, protocol number 164/2020.

2.8. In vitro immunomodulation assays

2.8.1. Obtaining splenocytes from mice

Splenocytes were obtained according to the methodology proposed by Cruz-Filho et al. [22] and Melo et al. [23] respectively. For this procedure, female mice (ages 7 to 8 weeks) of the BALB/c strain were used, after approval by the Animal Use Ethics Committee of Institute Aggeu Magalhães/Oswaldo Cruz Foundation, protocol number 164/2020. Initially, the animals were anesthetized with 10 mg/Kg xylazine hydrochloride and 115 mg/Kg ketamine and euthanized by cervical dislocation. Then the spleen of each mouse was aseptically removed and added to Falcon tubes containing RPMI 1640 with fetal bovine serum (complete medium). The spleens were submitted to a glass doucer homogenizer. Cell suspensions were transferred to Falcon tubes, layered with Ficoll-PaqueTM PLUS, density adjusted to 1077 *g*/mL, and centrifuged at 1000 x*g* at room temperature for 30 min. Mononuclear immune cells were recovered and washed twice with 1× PBS, followed by centrifugation at 500 x*g* for 10 min. Finally, they were resuspended in 2 mL of RPMI medium and cell concentration was determined in a Neubauer chamber.

2.8.2. Cell viability assays in lignin-stimulated splenocyte cultures

To evaluate the cytotoxicity promoted by lignins, the methodology proposed by Cruz-Filho et al. [22] and Melo et al. [23] respectively. Splenocyte cultures (10^6 cells/well) were treated with different concentrations of lignin dissolved in 1 % DMSO (100 to 6.25 μg/mL) for 24 h in a CO_2 cell oven. After this period, the cells were centrifuged, stained with propidium iodide (50 μM) and annexin V for 10 min and analyzed in flow cytometry (FACS Calibur platform) in 10,000 events. Data were analyzed in Flowing 2.0.1® software and graphs were plotted in GraphPad 5.0 software.

2.8.3. Cell proliferation analysis

The ability of splenocytes to proliferate against lignins was evaluated by the CFSE staining method, described by Cruz-Filho et al. [22] and Melo et al. [23] respectively. Splenocytes were treated for 24 h with lignin at concentrations of (100 to 6.25 μg/mL). The acquisition was performed on the FACS Calibur (BD®) platform and the results were analyzed in the Flowing 2.5.1® software and the graphs were plotted in the Prism 5.0® software.

2.8.4. Determination of cytokines and production of nitro oxide

Cytokines and nitric oxide were determined in the culture supernatants. Cytokines were determined by mouse cytometric bead array (CBA) kits for interleukins (IL)-2, -4, -6, -10, -17, tumor necrosis factor-α (TNF -α) and interferon- γ (IFN-γ) by flow cytometry. Nitric oxide was determined using the colorimetric method of Griess.

2.9. In vitro cytotoxicity assays against tumor cells

In this assay, cell viability was determined by the same methods as the MTT Method. This assay evaluated whether the lignins obtained had a toxic effect on tumor cell lines. Assays were performed according to Nerys et al. [48] with modifications. The following tumor cell lines were cultivated: MCF-7 (breast cancer), T-47D (breast cancer), Jurkat (leukemia/lymphoma), DU145 (human prostate cancer cell), and HepG2 (hepatoma).

These cells were cultured in RPMI 1640 medium (Gibco®), supplemented with 10 % fetal bovine serum and penicillin: streptomycin solution (1000 IU/mL:1000 μg/mL, 1 %). The cells were distributed into 96-well microplates and each well received 1×10^4 cells. These cells were incubated for 24 h in a humidified atmosphere oven at 37 °C with 5 % CO_2.

Then, the lignins were diluted in 1 % DMSO, the cells were added at different concentrations (100 to 1.5 μg/mL) and the plates were incubated again for 72 h under the same conditions described above. After 72 h, 20 μL of MTT (3-(4,5-dimethylazol2-yl)-2,5-diphenyl tetrazoline bromide) solution at a concentration of 5 mg/mL diluted in PBS (Phosphate Buffer) was added to each well. – Saline). The plates were protected from light and incubated once more in a humidified oven for 3 h. The absorbance reading was performed 24 h later at 570 nm in a plate reader (ELX808, Biotek, USA).

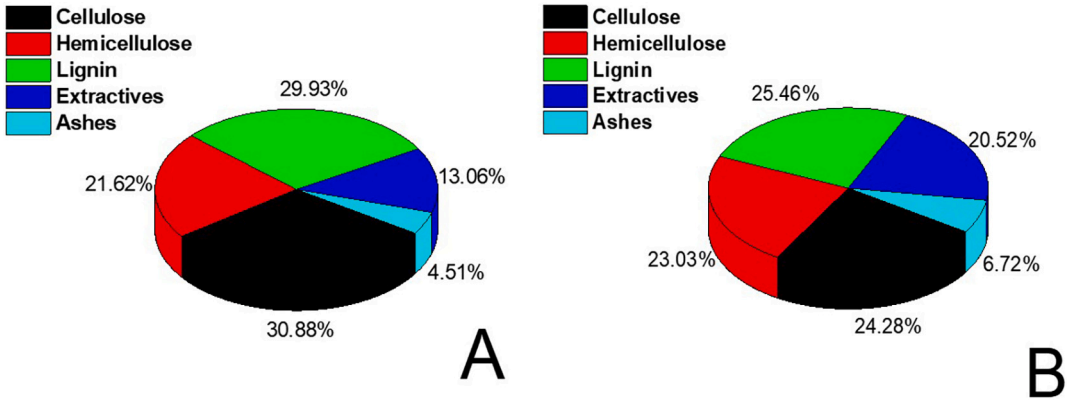

Fig. 1. Results of chemical composition analysis, cellulose, hemicellulose, lignin, extractives and ash contents for the branch (A) and leaves (B) of *Buchenavia viridiflora.*

Assays were performed in triplicate and included untreated controls (only cells and culture medium) and the standards amsacrine, asulacrine, and doxorubicin (diluted under the same conditions as lignins. Cell viability was determined using Eq. 5. IC_{50} values calculated by means of non-linear regression using GraphPad Prism 5 software. In addition, the selectivity index (IS) was determined for the ratio between IC_{50} values for normal cells and antitumor cells for the extract, amsacrine, asulacrin, and doxorubicin these values were determined using Eq. (7).

$$IS = \frac{IC_{50}\ \text{Normal cells}}{IC_{50}\ \text{Tumor cells}} \tag{7}$$

2.10. In vitro antimicrobial activity

2.10.1. Microorganisms evaluated and standardization of the inoculum

The microorganisms evaluated in this study were obtained from the Collection and Culture of Microorganisms, located at the Department of Antibiotics at the Federal University of Pernambuco (UFPEDA). Six bacterial strains were obtained: *Acinetobacter baumannii* UFPEDA-1024, *Enterococcus faecalis* UFPEDA-138, *Enterococcus faecalis* UFPEDA-69, *Staphylococcus aureus* UFPEDA-709, *Pseudomonas aeruginosa* UFPEDA-416, *Pseudomonas aeruginosa* UFPEDA-261. In addition to the bacterial strains, five yeast strains were evaluated: *Candida albicans* URM 95, *Candida albicans* 4664, *Candida albicans* UFPEDA-1007, *Candida guilliermondii* UFPEDA-6390, and *Candida glabrata* UFPEDA-6393. The standardization of the inoculum (bacteria and yeast) was performed following the documents of the Clinical Laboratory Standards Institute, M100 (CLSI, 2017) and M60 (CLSI, 2018), respectively.

The bacterial strains were cultivated in Mueller Hinton broth until reaching turbidity equivalent to the Mc Farland scale of 0.5. After growth, the samples were diluted in saline solution to obtain the final inoculum (1.5×10^7 CFU/mL). Yeasts were grown in RPMI 1640 broth and diluted in the sterile saline solution until turbidity was equivalent to 0.5 Mc Farland scale (1.0×10^6 to 5.0×10^6 CFU/mL).

2.10.2. Determination of the minimum inhibitory concentration (MIC) and minimum bactericidal or fungicidal concentration (MBC/MFC)

Assays to determine the minimum inhibitory concentration (MIC) and minimum bactericidal or fungicidal concentration (MBC/MFC) were performed according to the methodology proposed by Nerys et al. [48] with few modifications. Serial dilutions were performed in DMSO 1 % of the lignins and the standards (Gentamycin, Amikacin, Oxacillin, and Ampicillin+Sulbactam, against bacteria and Micafungin for yeasts), varying the concentration from 1024 to 4 μg/mL.

The 96-well plates were incubated for 24 h at 37 °C (bacteria) and 30 °C for 48 h (yeasts) respectively. 0.01 % (*w/v*) resazurin solution was used as an indicator of bacterial growth. Cultures were seeded on Mueller Hinton medium (Bacteria) or Sabourand Agar (yeasts) to determine MBC/MFC. Activity against the microorganism was considered when the MIC was ≤1024 μg/mL.

2.11. In vitro antiparasitic activity: cytotoxicity against Plasmodium falciparum (3D7) and Plasmodium falciparum (Dd2) strains

Lignins were evaluated for their *in vitro* antimalarial activity against the chloroquine-sensitive *Plasmodium falciparum* strain (3D7) that expresses GFP (green fluorescent protein) and the chloroquine-resistant Plasmodium falciparum strain (Dd2). The tests were carried out according to the methodology proposed by Lobo et al. [49] and Teixeira et al. [50] with modifications. Desynchronized culture with 0.6 % hematocrit and 0.5 % parasitemia was incubated in a 96-well flat-bottomed plate with concentrations ranging from 0.17 to 10,000 ng/mL for each lignin for 72 h (37 °C and 5 % CO_2).

The growth of the chloroquine-sensitive parasite was evaluated by flow cytometry (Beckman Coulter, Cytoflex) with a 96-well plate reader, using Fl-1 (green fluorescent protein [GFP]; excitation wavelength, 488 nm). Typically, 20,000 to 40,000 red blood cells (RBCs) were counted for each well. Samples were analyzed using FlowJo software (Tree Star Inc.). The resistant strain was previously stained with 0.5× SYBR green I (Invitrogen, Thermo Fisher Scientific) for 30 min in the absence of light at 37 °C, washed once with PBS, and then analyzed by cytometry under the same conditions. of the susceptible strain 3D7-GFP.

As standards, the drug chloroquine (for sensitive strain) and Dihydroartemisinin (DHA) (resistant strain) were used at the same concentrations as lignins. Cell viability results were determined by Eq. (5).

The IC_{50} was determined as the concentration that inhibited the growth of the parasite by 50 %. This parameter, obtained from non-linear regression, was determined using the GraphPad Prism 5 software (trial version). At least three experiments were performed, each in duplicate, to obtain the average IC_{50} presented. Chloroquine was used as a control drug.

2.12. Statistical analysis

Results are expressed as mean ± standard error of the mean (SEM). Statistical analysis was performed using analysis of variance (ANOVA) with Tukey's test to assess significant differences between groups. p values <0.05 were considered significant. All statistical analyzes were performed using GraphPad 5.0 software.

3. Results and discussion

3.1. Results of the analysis of the chemical composition of the branches and leaves of the species Buchenavia viridiflora, in addition to the lignin yield

Plants present in their chemical composition cellulose, hemicellulose, and lignin, together with a small content of ash (inorganic substances) and extractives (organic substances of low molecular weight) [15,20]. These components are present in the cell wall and present levels that may vary depending on age, developmental stage, type of plant species, plant region, extraction method, and quantification [20].

Fig. 1 presents the results of the analysis of the composition in percentage, for the constituents: cellulose, hemicellulose, lignin, extractives, and ash for the branches and leaves of *Buchenavia viridiflora*.

The composition results presented are different between the branches and the leaves. The branches showed higher levels of cellulose and lignin when compared to the leaves that presented higher levels of hemicellulose, extractives, and ash. After analysis of the composition, the branches and leaves were submitted to acid pretreatment, followed by alkaline delignification, and the black liquor obtained from the delignification was acidified to obtain lignin. The yield was 67.9 ± 1.1 % and 60.2 ± 0.3 % for the branch and leaf respectively. The results obtained show variations; however, higher yields were observed for the lignin of the branch when compared to the yields obtained for the leaves, this fact was expected due to the higher content of lignin present in the branch.

The literature presents different yield results for lignins. Arruda et al. [15], using the same production process (acid pretreatment followed by alkaline delignification) obtained a yield of 85.7 % for the lignin extracted from the *Crataeva tapia* leaves. Silva et al. [20] obtained a yield of 89.8 ± 1.7 % for lignin from the *Morinda citrifolia* leaves. Guo et al. [34] performing extraction under different experimental conditions obtained yields ranging from 44.10 to 74.14 %. Watkins et al. [51] extracted lignins from alfalfa fibers, pine straw, wheat straw, and flax fibers and obtained yields of 34 %, 22.65 %, 20.40 %, and 14.88 % respectively. Gilarranz et al. [35] obtained 80 % for wheat straw lignin. These values vary according to the source and the extraction and quantification method.

3.2. Physical and chemical characterization of lignins

3.2.1. Elemental analysis: carbon, hydrogen, nitrogen and oxygen contents

Elemental analysis is an important technique to determine the levels of different elements present in the lignin structure [36]. Therefore, it is possible to determine the contents of carbon (C), hydrogen (H), and nitrogen (N) [15,20]. The oxygen (O) content can be determined by analytical differences [15,20,37,38]. The results showed different results for the two lignins under study. For the lignin extracted from the branches, the following contents were obtained: carbon (61.46 ± 0.1 %), hydrogen (7.18 ± 0.3 %), nitrogen (0.33 ± 0.07 %) and oxygen (31.03 ± 1.0 %), while for the lignin extracted from the leaves were obtained: carbon (58.14 ± 0.5 %), hydrogen (6.20 ± 0.14 %), nitrogen (0.52 ± 0.01 %) and oxygen (35.14 ± 0.9 %).

Comparing the results obtained between the lignins of branches and leaves, it is clear that the elemental composition differs. It was observed that the lignin of the branches presented higher levels of carbon in its structure, which characterizes that its structural skeleton presents a hydrocarbon profile, which may or may not have aromaticity [15,20,37,38]. Another element highlighted was the oxygen, the leaves showed higher levels of oxygen when compared to the lignin of the branches, characterized by a less condensed and more oxygenated chemical structure. The lower nitrogen content is possibly due to contamination by nitrogen compounds present in the plant [37].

These differences are directly related to the region of the plant (branch or leaf) since the same process of obtaining was used, acid pretreatment followed by alkaline delignification [15,20,37,38]. Other authors also obtained different results for the contents of carbon, oxygen, nitrogen, hydrogen, and sulfur. El Mansouri and Salvadó [52] evaluated different lignins, they obtained values of carbon that varied between 58.34 and 65.00 %, oxygen from 44.14 to 28.24 %, hydrogen from 5.15 to 6.12 %, nitrogen from 0.02 to 1.26 % and sulfur 0.00 to 1.25 %. Guo et al. [53] also evaluated different lignins, they obtained values of carbon that varied between 60.70 and 68.06 %, oxygen from 23.23 to 33.15 %, and hydrogen from 4.62 to 6.31 %, nitrogen from 0 to 2.71 %, and sulfur 0.00 to 1.25 %. The authors also justify that the difference in the contents is directly related to the extraction method and source of obtaining.

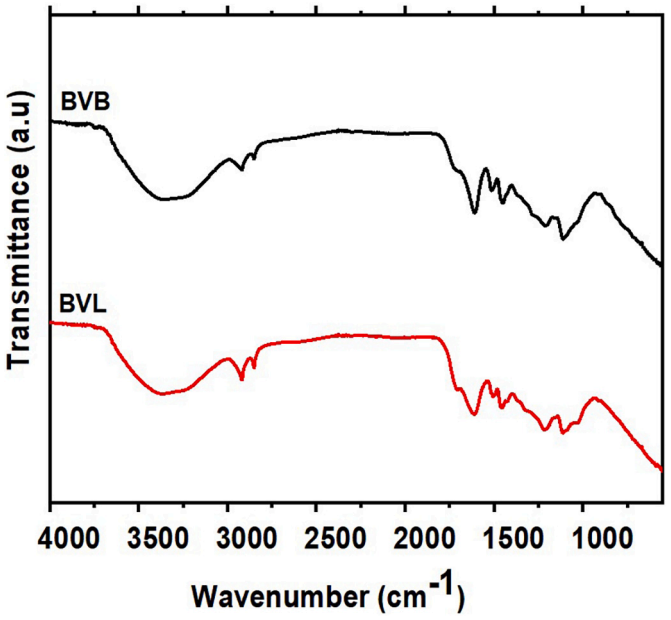

Fig. 2. Spectrum in the infrared region for the lignins of the branches (BVB) and leaves (BVL) of *Buchenavia viridiflora*.

3.2.2. Fourier transform attenuated total reflection spectroscopy (ATR-FTIR) and ultraviolet visible (UV/Vis) spectroscopy

The infrared absorption spectra, in the region of 4000 to 400 cm^{-1} for lignins obtained from the branches (BVB) and leaves (BVL) of *Buchenavia viridiflora*, are shown in Fig. 2. The bands were identified by comparison using bands obtained by Santos et al. [19], Melo et al. [23], Arruda et al. [15], and Silva et al. [20] characterizing different alkaline lignins.

According to the spectra, characteristic lignin bands are observed. Broad bands between 3440 and 3410 cm^{-1} can be observed referring to intra and intermolecular hydrogen bonds (stretching or axial deformation O—H) [19,20]. The bands corresponding to 2980–2900 cm^{-1} correspond to the stretching of C—H bonds of aliphatic groups (saturated hydrocarbons). Although this group is present in the lignins of this study, in each of them it appears with a different intensity and enlargement, suggesting different aliphatic groups and in different amounts in each of the samples [23]. The bands between 1709 and 1700 cm^{-1} refer to C═O stretching in unconjugated ketones, carbonyls, and ester groups. The bands referring to the vibrations of the aromatic skeleton are close to 1600 and 1505 cm^{-1}. The bands between 1450 and 1454 cm^{-1} refer to the deformation of the C—H bonds in methyl groups [19,20,23].

The bands between 1367 and 1360 cm^{-1} refer to the C—H aliphatic stretch in CH_3, and O—H phenolic stretch. The bands of 1260–1230 cm^{-1} refer to the angular deformations of the O—H bonds, and C—O bonds of guaiacyl rings (G) [20]. The bands at 1163–1160 cm^{-1} refer to the C═O stretching in conjugated ester groups, present in the guaiacyl

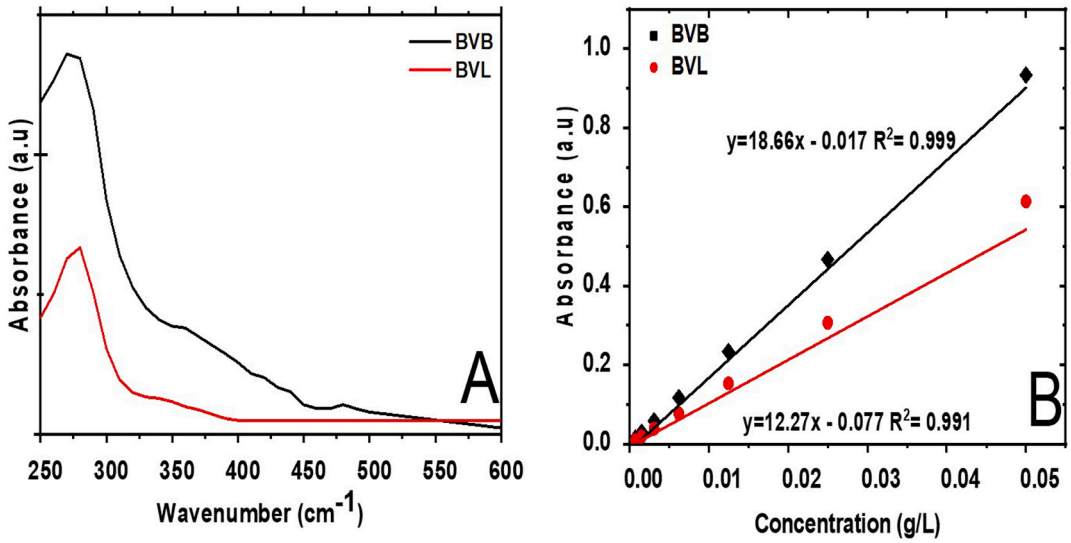

Fig. 3. Spectrum in the UV/vis region (A) and the curves for the determination of absorptivity (B) for the lignins under study.

(G), syringyl (S), and *p*-hydroxyphenyl (H) units. The bands found in the region between 1120 and 1125 cm^{-1} refer to the aromatic ring (typical of syringyl) [19,20].

Close to 1040–1020 cm^{-1} there are bands related to deformation in the aromatic C—H plane and C—O deformation in primary alcohols, this band reveals that these lignins have higher contents of guaiacyl units when compared to syringyl units [15,20]. At 875–870 cm^{-1}, bands related to aromatic C—H bonds appear (out-of-plane deformation of C—H in *p*-hydroxyphenyl unit) [15,19,20,23]. Close to 1040–1020 cm^{-1} there are bands related to deformation in the aromatic C—H plane and C—O deformation in primary alcohols, this band reveals that these lignins have higher contents of guaiacyl units when compared to syringyl units [15,20]. At 875–870 cm^{-1}, bands related to aromatic C—H bonds appear (out-of-plane deformation of C—H in *p*-hydroxyphenyl unit) [15,19,20,23].

In addition to the infrared analysis, a UV–Vis spectroscopy study was also carried out. UV–Vis spectroscopy is an important technique to assess the aromatic nature of lignin [39,40]. Due to the different chromophore groups existing in the macromolecular structure, the UV–vis analysis shows us the presence or absence of functional groups, but we cannot predict the structures [39]. However, it is an important tool for determining the purity and verifying the presence of its main cinnamyl acids [39,40]. Fig. 3A shows the spectra of lignins obtained from leaves and branches of *Buchenavia viridiflora*. In addition, Fig. 3B shows the concentration lines as a function of absorbance to obtain the extinction coefficient.

The results obtained in Fig. 3A were compared to those obtained by Lee et al. [39] and Skulcova et al. [40]. The band between 250 and 280

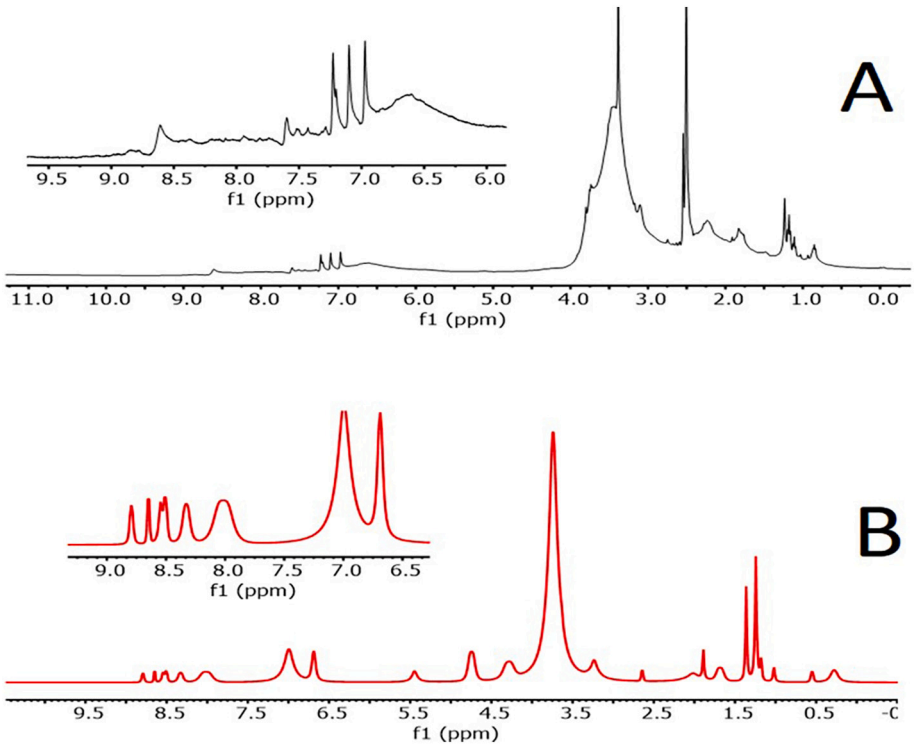

Fig. 4. ^{1}H NMR spectra for acetylated lignins from branches (A) and leaves (B) of *Buchenavia viridiflora* dissolved in deuterated DMSO ($DMSOd_6$).

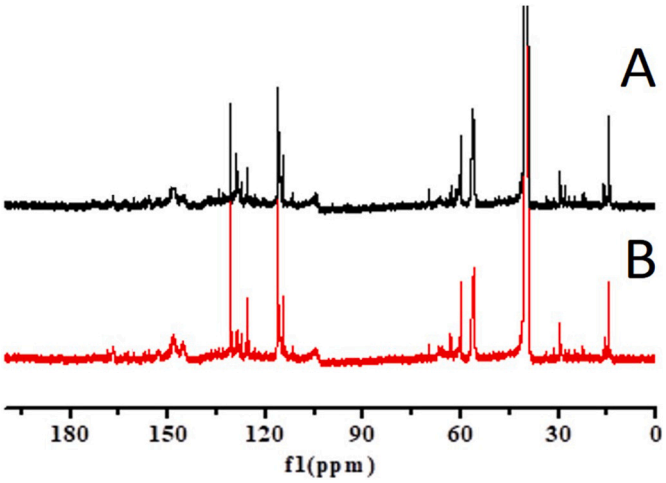

Fig. 5. ^{13}C NMR spectra for acetylated lignins from branches (A) and leaves (B) of *Buchenavia viridiflora* dissolved in deuterated DMSO ($DMSOd_6$).

nm is related to chromophore groups of conjugated and unconjugated phenolic compounds, in addition, the maximum absorbance having occurred at 280 nm, confirms as well as in the FTIR that there is a greater number of guaiacyl-type units in syringyl groups would have the closest band at 270 nm. The absorptivity (Fig. 3B) obtained for the lignin from the branch was 18.66 L/g/cm and the molar absorptivity obtained for the leaf was 12.27 L/g/cm.

Other authors also obtained results of absorptivity close to those obtained by ours characterizing alkaline lignins. Silva et al. [20] obtained 16.7 L/g/cm for lignin obtained from the *Morinda citrifolia* leaves. Arruda et al. [15] obtained 12.8 L/g/cm for lignins from *Crataeva tapia* leaves. Melo et al. [23] obtained 22.27 L/g/cm for lignin from the *Caesalpinia pulcherrima* leaves. Rocha et al. [54] for sugarcane bagasse lignin 14.6 L/g/cm.

These differences in absorptivity are associated with the degree of condensation and substitution of these lignins. The greater the number of substituted rings, the greater the absorptivity at 280 nm [15,20,23,54].

3.2.3. Analyzes by nuclear magnetic resonance spectroscopy (^{1}H NMR, ^{13}CNMR and ^{1}H—^{13}C HSQC)

Nuclear Magnetic Resonance (NMR) analyses are important and widely used tools for investigating the chemical structure of different lignins [15,20,23,54]. The ^{1}H NMR analysis is one of the techniques frequently used in the study of structural characterization of lignin, both qualitatively and quantitatively, in addition to being easy to perform [15,20,23]. Thus, it is possible to determine different protons, which belong to the groups, carboxylic and aldehyde, aromatic and vinylic, β-vinyl and benzyl, methoxylic, and other hydrogens linked to the C3 chain, such as α, β, and γ, aromatic acetoxy, aliphatic acetoxy and aromatic acetoxylic ortho to biphenyl bond, highly shielded aliphatic, among others [54]. The presence of these groups is related to the type of lignin and the extraction method [15,20,23,54].

Fig. 4 shows the ^{1}H NMR spectrum of acetylated lignins from branches (Fig. 4A) and leaves (Fig. 4B) of *Buchenavia viridiflora* dissolved in deuterated DMSO. The signals present in the two structures were previously identified by Rocha et al. [54], Melo et al. [23], Arruda et al. [15], and Santos et al. [19] characterizing different lignins.

Signals found in the region of 9.0–7.0 are attributed to aromatic protons ortho to carboxylic groups, formyl protons in cinnamaldehyde and benzaldehyde-like substructures, and protons located ortho to a carbonyl group on benzaldehyde units [15,20,23]. Signals with a chemical shift around 7.0 ppm are attributed to the protons of the aromatic ring of alcohols (*p*-coumaryl, coniferyl, and sinapyl) and vinylic protons [15,23]. In the region at 6.5–7.0 ppm signals are assigned to aromatic protons in propanesyringyl and propaneguaiacyl units.

Side chain protons from syringyl units in the 6.61 ppm region [54]. The hydrogens attached to the α and β carbons show signs at 5.1 and 4.7 ppm, respectively [15,23]. The signals at 4.2 and 4.4 ppm are represented by the Hγ of various lignin units [23]. It is still possible to verify signs of hydrogens attached to the carbons of the propanoid chain, as in 4.13 ppm, referring to Hβ in Cβ in β-O-4 bond, and in 5.33 ppm referring to Hα in phenylcoumaran structures [15,20,23]. A signal characteristic of methoxyl protons is observed at 3.65 ppm [54]. Signals between 3.1 and 3.20 ppm are characteristic of H-β, in β—β structures. The displacement signal around 2.5 ppm refers to the DMSO solvent, respectively [15,20,23]. The signals at 1.60 ppm and 2.60 ppm originate from aliphatic and phenolic hydroxyl groups, respectively [15,20,23,54]. Signals <1.60 ppm are related to CH_3 and CH_2 groups in saturated aliphatic chains [54].

The ^{13}C NMR spectra are useful in the elucidation of the carbonic structure of different lignins [19,22,23,55]. The ^{13}C NMR spectrum can be divided into different regions, at 200 to 165 ppm it contains signals attributed to carbonyl carbons; in the region, em165 to 100 ppm signals are attributed to aromatic and olefin carbons; and a last one between

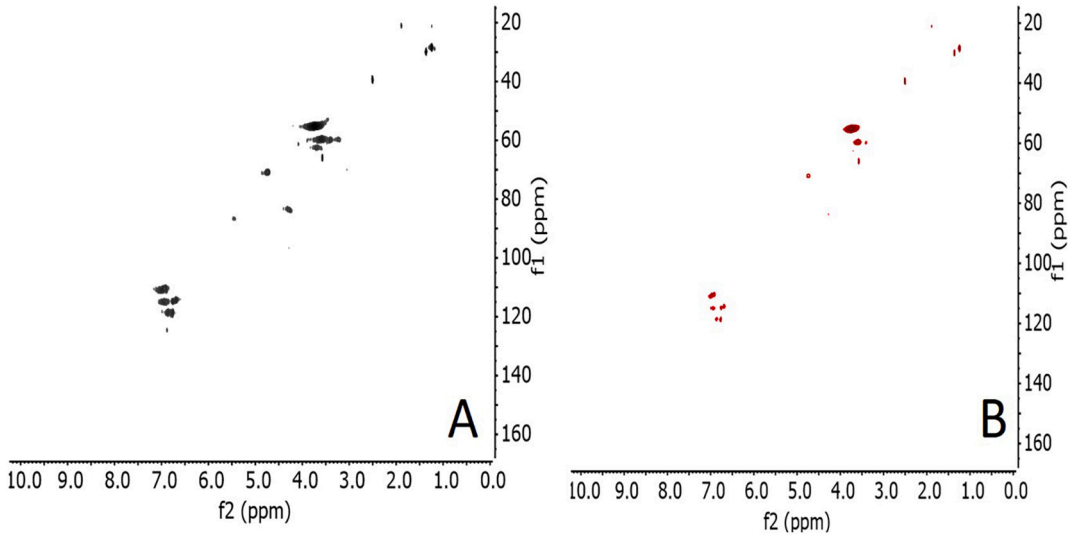

Fig. 6. 2D-HSQC NMR spectra for acetylated lignins from branches (A) and leaves (B) of *Buchenavia viridiflora* dissolved in deuterated DMSO ($DMSOd_6$).

Table 1
Assignment of the main $^{13}C—^{1}H$ cross signals in the HSQC NMR spectra to the acetylated lignins of the branches (BVB) and leaves (BVL) of *Buchenavia viridiflora*.

Labels	Lig. BVB δ_C/δ_H (ppm)	Lig. BVL δ_C/δ_H (ppm)	Assignment
Bβ	52.9/3.47	53.4/3.48	Cβ-Hβ in β-β resinol substructures (B)
OMe	55.6/3.72	55.1/3.75	C-H in methoxyls
Aγ	59.52/3.60	59.62/3.60	Cγ-Hγ in β-O-4 substructures (A)
Iγ	61.50/3.98	61.9/3.99	Cγ-/Hγ in p-hydroxycinnamyl alcohol end-group (I)
X5	64.28/3.57	Nd	C5-H5 in β-D-Xylopyranoside (X)
Bγ	71.75/4.133	Nd	Cγ-Hγ in β-β resinol substructures (B)
Aβ (S)	83.985/4.399	83.74/4.27	Cβ-Hβ in β-O-4 substructures linked to S (A)
S′2,6	107.0/7.1	107.0/7.1	C2,6-H2,6 in oxidized (Cα = O) phenolic syringyl units (S′)
G2	111.0/7.0	111.0/7.0	C2-H2 in guaiacyl units (G)
G5	115.5/6.71	114.73/6.76	C5-H5 in guaiacyl units (G)
G6	119.7/6.79	118.62/6.77	C6-H6 in guaiacyl units (G)

A: *β-O-4′* linkages; B: resinol structures (*β-β′*); G: guaiacyl units; S: syringyl units; X:Xylopyranoside; I: *p*-hydroxycinnamyl; Lig: lignin. Nd: Not determined.

100 and 10 ppm where the signals are assigned to aliphatic carbon atoms [19,23,55]. Fig. 5 shows the ^{13}C NMR spectrum of acetylated lignins from branches (Fig. 5A) and leaves (Fig. 5B) of *Buchenavia viridiflora* dissolved in deuterated DMSO.

The signals present in the two structures were previously identified by Melo et al. [23], Arruda et al. [15], and Santos et al. [19].

The ^{13}C NMR spectra were very similar for the two lignins. The chemical shift at 30.0 ppm refers to the α and β carbons of methylene groups, not linked to oxygen, in the propanoid chain. The signals below found in the region below 30 ppm are attributed to unsubstituted aliphatic due to methyl-terminal groups [22,23]. The signal at 40 ppm refers to the deuterated DMSO solvent [55]. The presence of methoxyl groups is verified in the displacement of 57.0 ppm, since the displacement range of -OCH_3 groups is from 55 to 57 ppm [22].

The signals in the region between 73 and 60 ppm refer to the displacement of CγOH and Cγ-OH with binding to Cβ of the β-O-4 type, respectively [22]. From 110 to 170 ppm is the carbon region in the aromatic skeleton [19,22,23,55]. The shift at 112 ppm is related to the C2 and 115 ppm to the C5 of the guaiacyl unit, at 130 and 134 ppm to the C1 of the guaiacyl ring and syringyl [15,55]. At 148 ppm the displacement refers to the C3 and C4 of the guaiacyl ring and the non-etherified C3 and C5 of the syringyl and *p*-hydroxyphenyl rings [19,23,55].

In the ^{1}H and ^{13}C (1D) NMR analyses, despite being efficient for the elucidation of lignins, the spectra obtained may present overlapping signals, requiring the use of more refined analyzes [56,57]. Therefore, single heteronuclear quantum coherence spectroscopy of 2D-HSQC (Heteronuclear single quantum coherence spectroscopy), provides lignin structural information in greater detail and with less ambiguity [57].

Fig. 6 shows the 2D-HSQC NMR spectrum of acetylated lignins from branches (Fig. 6A) and leaves (Fig. 6B) of *Buchenavia viridiflora* dissolved in deuterated DMSO. The signals present in the two structures were previously identified by Zeng et al. [56], Zhao et al. [57], and Silva et al. [20].

The 2D-HSQC NMR spectrum for the lignins under study showed two important regions: the aromatic region or region I ($\delta C/\delta_H$ 105–140/5.5–8.0 ppm) and the oxygenated aliphatic region or region II ($\delta C/\delta_H$ 50–105 /2.5–5.5 ppm). The attributions of the main correlations of the acetylated lignin samples are listed in Table 1. These correlation results were previously determined by other authors Zeng et al. [56], Zhao et al. [57], and Silva et al. [20] different lignins.

The results show that the two lignins present a predominance of guaiacyl units, corroborating the results obtained by the spectroscopic analyzes carried out in this work. In addition, the lignin obtained from the branches showed a signal of carbohydrate residues ($\delta C/\delta_H$ 64.28/3.57 ppm).

3.2.4. *Thermal Analysis: thermogravimetry (TG), derived thermogravimetry (DTG) and Differential Scanning Calorimetry (DSC)*

Thermoanalytic techniques have been defined as methods in which the variation of a certain physical property of a sample is measured as a function of time or temperature [58–60]. In thermogravimetric analysis, the variation of mass as a function of temperature is measured, as shown in the thermograms in Fig. 7. It can be noted that the thermograms show a gradual displacement of the curves towards higher temperatures, with increasing heating rates. This phenomenon is expected because the low heating rates generate large time intervals to generate the respective curves [58–60]. Fig. 7A presents the curves obtained by thermogravimetric analysis (TGA), whereas Fig. 7B presents the DTG curves (thermogravimetric derivative). For lignins obtained from the branches and leaves of *Buchenavia viridiflora.*

The thermal decomposition of lignin is a complex mechanism that involves several bond-breaking reactions [58–60]. Studies report that this degradation can occur over a wide temperature range from 200 to

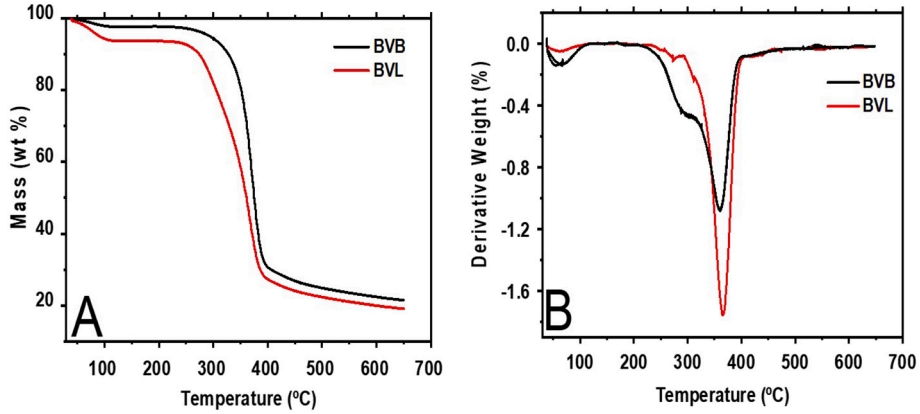

Fig. 7. Thermogravimetric curves (TGA) (A) and the first derivative of mass loss (DTG) (B) for the lignins in this study.

Table 2
Values of mass loss in percentage for each of the thermal degradation events, maximum degradation temperature obtained by DTG and percentage of residual mass for the lignins of the branches (BVB) and leaves (BVL) of *Buchenavia viridiflora*.

Lignin	T_{P1} (° C)	Mass (%)	T_{P2} (° C)	Mass (%)	T_{P3} (°C)	Mass (%)	Residual mass (%)
BVB	67.4	3.9	287.7	16.6	362.7	60.64	18.86
BVL	64.1	3.7	Nd	Nd	366.0	74.85	21.45

T_P: Peak temperature at each degradation event determined by DTG, Nd: not determined.

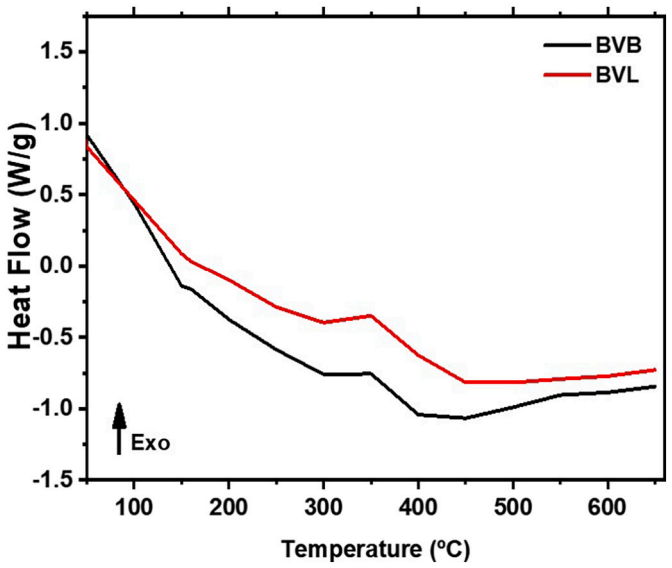

Fig. 8. Results of differential scanning calorimetry (DSC) analysis for lignins from branches and leaves of *Buchenavia viridiflora*.

700 °C [15,20,23,58,59]. The lignins presented different thermal behavior, the branch lignin presented three prominent thermal events, while the leaf lignin presented two events. These events are confirmed by the DTG curves (Fig. 7B).

Degradation ranges were obtained by comparison to Naron et al. [58], Torres et al. [59], Melo et al. [23], Arruda et al. [15], and Silva et al. [20] evaluating different lignins.

Initially, in the temperature range between 50 °C and 120 °C, there is a mass loss of approximately that can be attributed to the dehydration of the sample. This can be suggested because after this event the mass remains unchanged until the temperature of 250 °C. Between 250 °C and 315 °C, mass loss occurs, resulting in non-lignin compounds, such as polysaccharides and alcohols, and aliphatic acids (corroborating the 2D-HSQC NMR spectrum), in addition to the cleavage of β-O-4 bonds. This event was observed only in the branch lignin. In the range from 320 to 450 °C, the DTG presented a well-defined peak, characterizing the end of the most intense variation of mass loss. In this temperature range, it is believed that lignin degradation occurs through condensation and polymerization, that is, degradation of the aromatic ring and the guaiacyl, syringyl, and *p*-hydroxyphenyl units into monomeric phenols, aldehydes, alcohols, and acids. At temperatures above 450 °C, no significant variations in the mass loss were observed.

Table 2 presents the mass loss in percentage for each of the events presented for the lignins obtained from the branches (BVB) and leaves (BVL) of *Buchenavia viridiflora*.

This maximum degradation temperature is characteristic of lignins. Watkins et al. [51] extracted lignins from alfalfa fibers, wheat straw, pine straw, and flax fibers and obtained a maximum degradation temperature of 331.87 °C, 328.50 °C, 336.11 °C, 332.44 °C respectively.

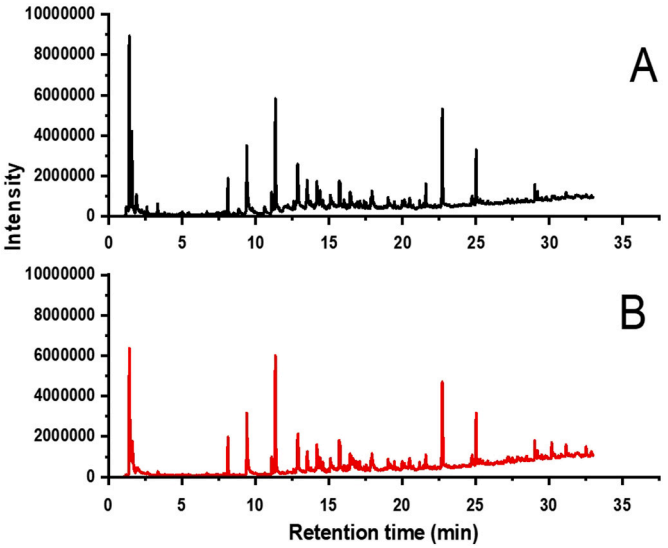

Fig. 9. Py-GC / MS chromatograms of lignins obtained from branches (A) and leaves (B) and from *Buchenavia viridiflora*.

Silva et al. [20] evaluating lignin obtained from the *Morinda citrifolia* leaves, obtained maximum degradation at a temperature of 350 °C. Arruda et al. [15] obtained a maximum thermal decomposition temperature of 350 °C for the lignin extracted from the *Crataeva tapia* leaves. Naron et al. [58] evaluated different technical lignins, they obtained maximum thermal degradation in a range of 370–390 °C.

In addition to the thermogravimetric analyses, differential scanning calorimetry analyzes were performed (Fig. 8) for the lignins of the branches and leaves of *Buchenavia viridiflora*. Fig. 8 showed an endothermic event (associated with water loss), which occur between 30 and 150 °C, and an exothermic event (due to lignin degradation), between 300 and 400 °C. These results corroborate those obtained by the TGA/DTG curves (Fig. 7).

Other authors obtained a DSC profile for different lignins similar to those obtained for the lignins in this study. Among these we can mention, Watkins et al. [51] analyzed lignins derived from alfalfa, pine straw, and flax fiber. Arruda et al. [15] and Silva et al. [20] for the lignins obtained from the leaves of *Crataeva tapia* and *Morinda citrifolia* respectively.

3.2.5. Pyrolysis coupled to GC/MS lignin of branches and leaves of Buchenavia viridiflora

Analytical pyrolysis can be defined as a technique for characterizing lignins by chemical degradation reactions, induced by thermal energy, in the absence of oxygen, resulting in a set of small molecular species, which are related to the composition of the original sample [61]. The possibility of gas chromatography to separate the products from pyrolysis and mass spectrometry to identify them makes the association between these techniques a powerful tool for the characterization of several non-volatile polymeric materials [61,62].

The compounds resulting from the thermal degradation of alkaline lignins (branches and leaves) were mainly monomeric aromatic products with phenolic hydroxyl and aromatic methoxyl groups, depending on the different bonds between the individual lignin units [20,61,62]. The pyrolysis products identified correlated well with the lignin structure, due to the decomposition of the polymer precursor compounds, *p*-hydroxyphenyl, guaiacyl, and syringyl monomers, due to the breaking of β —O— 4, α–O–4, C—C existing in the molecule, thus producing a large number of phenolic structures [20,61]. The formation of phenolic compounds and low molecular weight volatile species is explained by chain reactions with cleavage of side chains such as $–OCH_3$ and –OH in the aromatic ring [20,61,62].

Table 3
Relative distribution of the peak area of the main products for the lignins of the branches (BVB) and leaves (BVL) of *Buchenavia viridiflora* in Py-GC/MS.

RT/min	Product compounds	Formula	Origin	BVB area	BVB relative percentage (%)	BVL area	BVL relative percentage (%)
2.3	Benzene	C_6H_6	Aromatic	988,165	3.62	1,928,994	6.64
3.3	Toluene	C_7H_8	Aromatic	597,633	2.19	384,615	1.32
5.0	xylene	C_8H_{10}	Aromatic	0.00	0.00	0.00	0.00
7.4	Phenol	C_6H_6O	H-lignin	0.00	0.00	0.00	0.00
9.2	4-methylphenol	C_7H_8O	H-lignin	1,538,461	5.64	1,875,739	6.46
9.5	Guaiacol	$C_7H_8O_2$	G-lignin	1,923,076	7.05	3,075,739	10.59
10.9	4-ethylphenol	$C_8H_{10}O$	H-lignin	763,313	2.80	934,911	3.22
11.4	4-methylguaiacol	$C_8H_{10}O_2$	G-lignin	5,792,899	21.23	5,798,816	19.96
11.7	catechol	$C_6H_6O_2$	Catechol	1,485,207	5.44	1,378,698	4.75
12.7	3-methoxycatechol	$C_7H_8O_3$	Catechol	2,366,863	8.67	2,041,420	7.03
13.0	4-ethylguaiacol	$C_9H_{12}O_2$	G-lignin	2,313,609	8.48	1,928,994	6.64
13.5	4-vinylguaiacol	$C_9H_{10}O_2$	G-lignin	1,650,887	6.05	1,159,763	3.99
14.2	Syringe	$C_8H_{10}O_3$	S-lignin	137,898	0.51	1,591,715	5.48
14.4	4-propylguaiacol	$C_{10}H_{14}O_2$	G-lignin	1,153,846	4.23	769,230	2.65
15.8	4-(1-propenyl)-guaiacol	$C_{10}H_{12}O_2$	G-lignin	1,485,207	5.44	1,656,804	5.70
16.4	Acetovanilone	$C_9H_{10}O_3$	G-lignin	1,207,100	4.42	1,159,763	3.99
17.1	3-acetonylguaiacol	$C_{10}H_{12}O_3$	G-lignin	1,094,674	4.01	881,657	3.04
18.1	4-(2-propenyl)-syringol	$C_{11}H_{14}O_3$	S-lignin	1,207,190	4.42	994,082	3.42
19.0	Syringaldehyde	$C_9H_{10}O_4$	S-lignin	875,739	3.21	715,976	2.46
19.9	4-ethanoylsyringol	$C_{10}H_{12}O_4$	S-lignin	710,059	2.60	769,230	2.65

RT: Retention time; G: guaiacyl units; H: *p*-hydroxyphenyl units; S: syringyl units.

Table 4
Results of the molecular distribution of lignin from branches (BVB) and leaves (BVL) of *Buchenavia viridiflora*.

Lignins	Mw (Da)	Mn (Da)	Mw/Mn
BVB	3945.10	2000.92	2.0
BVL	984.77	691.50	1.4

Py-GC/MS chromatograms of lignins from branches and leaves of *Buchenavia viridiflora* are shown in Fig. 9 and the identified compounds are shown in Table 3. The signals were previously identified by Wang et al. [63,64], Guo et al. [53], and Silva et al. [20] evaluating different alkaline lignins.

Pyrolysis coupled to GC/MS lignin aims to add more information about the chemical structure of lignins which in many cases could not be observed in other spectroscopic analyses [20,61,62] [53].

Thus, through this technique, it was possible to determine the percentage contents of aromatics, catechol, and G, S, and H units (calculated by the percentage presented in Py-GC/MS) present in the lignin structure of this study. The lignin obtained from the branches presented the following contents: aromatic = 5.81 %; catechol = 14.10 %; G = 60.91 %; S = 10.74 and H = 8.44 %. On the other hand, the lignin of the leaves presented the following aromatic contents = 7.96 %; catechol = 11.78 %; G = 56.56 %; S = 14.02 % and H = 9.68 %.

These results allowed us to conclude that the lignins obtained from the branches and leaves of this study can be classified with GSH with a predominance of G units. These results corroborate the results obtained in the spectroscopic analyzes carried out in this study.

Lignins have different levels of G, S, and H units and these vary according to the extraction and acquisition method, and source and quantification technique. The literature presents different works with the determination of these units by pyrolysis coupled to GC/MS, among these we can mention those carried out by Lourenço et al. [65] who obtained for the lignin of *Tectona grandis* the following contents 56.0 % of the G units, 42.2 % of the S units and 1.8 % of the H units, the authors classified this lignin as GS type.

Marques and Pereira [66] evaluating the composition of lignins obtained from cork tissues (stoppers) of *Betula pendula*, *Quercus suber*, and *Quercus cerris* observed predominantly a guaiacyl-based lignin: guaiacyl units (G) represented 85.7 %, 96.4 % and 93.7 % of lignin, respectively. in *B. pendula*, *Q. suber* and *Q. cerris* corks, while the syringyl (S) units totaled, respectively, 11.9 %, 2.5 %, and 2.7 %, and *p*-hydroxyphenyl (H) units for 2.4 %, 1.1 %, and 3.6 %. The pyrolysis of the woods of these same species confirmed the GS character of their lignins in contrast to the G-lignin-type stoppers.

Sequeiros and Labidi [67] evaluating lignins from industrial waste, they obtained different contents of G, S and H units for the organosolv lignins from olive trees (G = 26.07 %; S = 68.67 % and H = 5.26 %), eucalyptus kraft lignin (G = 23.80 %; S = 75.70 % and H = 0.49 %), acetosolv lignin from apple tree (G = 27.72 %; S = 64.54 % and H = 7.25 %), acetosolv lignin from formosolv almond shell (G = 45.43 %; S = 53.74 % and H = 0.83 %).

3.2.6. Molecular weight determination by gel permeation chromatography (GPC)

Molecular mass and molar mass distribution are important parameters in the study of the structure and properties of lignin [54,68]. The main method for obtaining information about the molar mass distribution is gel permeation chromatography [68] important to emphasize that although the GPC technique is widely used for the analysis of lignin fractionation, the information obtained by them refers only to the molecular volume, not allowing, therefore, any conclusion regarding the chemical composition of this macromolecule [23,54,68].

Table 4 presents the results obtained by the GPC for the lignins of the branches (BVB) and leaves (BVL) of *Buchenavia viridiflora*.

The results presented in Table 4 show that the lignins of the branches presented higher values of numerical average mass (Mn) and weighted average molar mass (Mw) when compared to the lignin of leaves. These values strongly contribute to the reactivity of lignins, that is, lignins that have lower Mn and Mw values (in this case leaf lignin) have high levels of phenolic and aliphatic hydroxyls, suggesting that in the extraction process there were cleavages of ether-type bonds. For lower molecular weight structures. The low levels of polydispersity show that these lignins present fragments with low heterogeneity in terms of molecular weight. In addition, the lignins in this work are of low molecular weight with values <4000 Da [54,68].

The literature presents different molecular weight values for alkaline lignins. Silva et al. [20] evaluated lignin from the *Morinda citrifolia* leaves, they obtained weight average molecular weight (Mw) of 2995 Da, a numerical average molecular weight (Mn) of 1762 Da, and a polydispersity value of 1.7. Arruda et al. [15] showed that the lignin from the *Crataeva tapia* leaves had a weight average molecular weight (Mw) of 1246.8 Da, a numerical average molecular weight (Mn) of 831.2 Da, and a polydispersity value of 1.5. Melo et al. [23] obtained the lignin from the *Caesalpinia pulcherrima* leaves, average molecular weight (Mw) of 2503 Da, numerical average molecular weight (Mn) of 1472 Da,

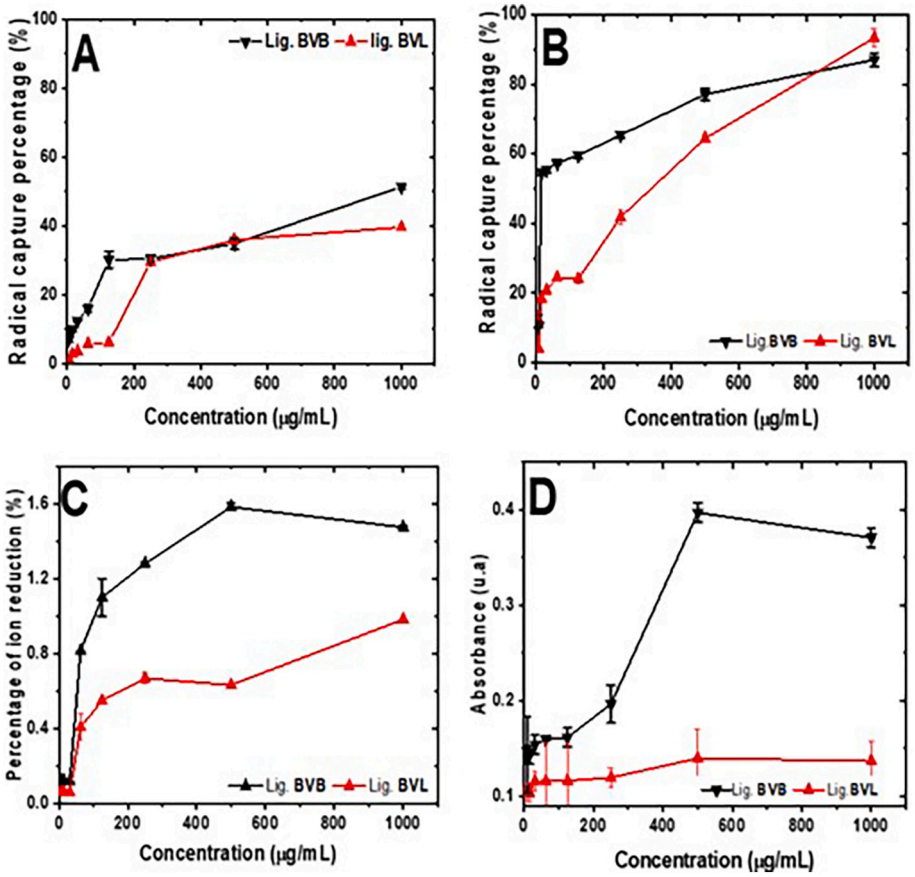

Fig. 10. Antioxidant activity promoted by lignins from branches (BVB) and leaves (BVL) of *Buchenavia viridiflora*. by different tests. Capture of DPPH (A), ABTS (B) radicals and reduction of molybdenum (C) and iron ions (D).

Table 5
Results of *in vitro* antioxidant activity promoted by lignins from branches (BVB) and leaves (BVL) of *Buchenavia viridiflora.*

Lignins	Radical DPPH•		Radical ABTS +		Reduction Mo^{6+} - Mo^{5+}		Reduction Fe^{3+}- Fe^{2+}	
	%	IC_{50} (µg/mL)	%	IC_{50} (µg/mL)	%	IC_{50} (µg/mL)	%	IC_{50} (µg/mL)
BVB	51.29 ± 0.1	884.56 ± 1.4	87.06 ± 0.15	14.08 ± 0.5	1.4 ± 0.01	Nd	37	Nd
BVL	39.55 ± 0.0	Nd	93.43 ± 0.1	350. 20 ± 1.6	0.9 ± 0.01	Nd	13	Nd
Ascorbic acid	99.8	7.75 ± 0.0	99.0	13.4 ± 0.0	98.0	5.34 ± 0.5	90.0	26.49 ± 0.3
(BHT)	99.1	18.9 ± 0.0	100	5.24 ± 0.02	94.0	8.85 ± 0.1	70.0	5.30 ± 0.1

Mean ± Standard deviation, %: Percentage at a concentration of 1000 µg/mL, BHT: Butylated hydroxytoluene, Nd: not determined at the concentrations studied.

and polydispersity value of 1.7.

Santos et al. [19] evaluated lignin from the *Conocarpus erectus* leaves, they obtained an average molecular weight of 2709 Da, a numerical average molecular weight of 1279 Da, and a polydispersity index value of 2.1. El Mansouri et al. [69] evaluated different alkaline lignins, they obtained weight average molecular weight (Mw) ranging from 1069 and 1746 Da, numerical average molecular weight (Mn) ranging from 675 and 1501 Da, and polydispersity value ranging from 1.16 to 1.39. Mao et al. [70] evaluating alkaline lignins from *Carex meyeriana* Kunth obtained weight average molecular weight (Mw) ranging from 1240 and 4590 Da, numerical average molecular weight (Mn) ranging from 1020 and 4120 Da, and polydispersity values ranging from 1.07 to 1.26.

These results confirm that the molecular weight of lignins is related to the process of extracting and obtaining lignins.

3.3. Total phenolic content and evaluation of the in vitro antioxidant activity

The results of the quantification of the phenolic groups present in the chemical structures of the lignins of the branches and leaves of *Buchenavia viridiflora*. Were expressed in equivalent grams of gallic acid per gram of lignin (GAE/g). The values obtained were 237.936 ± 2.533 and 166.519 ± 2.171 mg GAE/g for branch and leaf, respectively.

The literature reports different values of phenolic content present in lignins. Santos et al. [19], Melo et al. [23], Arruda et al. [15], and Silva et al. [20] obtained lignins from leaves of *Conocarpus erectus*, *Caesalpinia pulcherrima*, *Crataeva tapia* and *Morinda citrifolia* values of 465.90 ± 1.07, 41.33 ± 0.65, 189.6 ± 9.6 and 193.3 ± 2.7 GAE/g respectively. Cruz-Filho et al. [22] determining the content of phenolic compounds in the lignins of *Opuntia ficus-indica* and *Opuntia cochenillifera* obtained 36.4 ± 0.4 and 87.8 ± 6.5 mg GAE/g.

These results show that the contents of phenolic groups can vary according to the species from which the lignin is obtained, in addition to

Table 6
IC_{50} values for different alkaline lignins compared to the lignins obtained in this study.

Lignins	IC_{50} (μg/mL)	References
Buchenavia viridiflora branch	14.08 ± 0.5	This work
Buchenavia viridiflora leaves	350. 20 ± 1.6	This work
Acacia nilótica wood	2.84 a 3.95	Aadil et al. [73]
Prickly pear cladodes of *Opuntia cochenillifera*	253.9	Cruz-filho et al. [22]
Conocarpus erectus leaves	356.03	Santos et al. [19]
Caesalpinia pulcherrima leaves	251.34	Melo et al. [23]
Crataeva tapia leaves	430 ± 1.9	Arruda et al. [15]
Morinda citrifolia leaves	175.34 ± 1.3	Silva et al. [20]

the extraction and obtaining methods [71,72]. The phenolic groups present in the structure have become the focus of several types of research due to their biological properties, especially when it comes to their use as a natural antioxidant [72].

Fig. 10 and Table 5 present the curves and results of antioxidant activity for the lignins evaluated in this study.

The curves presented in Fig. 10 show that the antioxidant activity promoted by the lignins under study increased with increasing concentration. The results presented in Table 4 showed the activity values at the highest concentration studied (1000 μg/mL) and that the lignins presented IC_{50} (concentration capable of capturing radicals in 50 %) for the ABTS assay. This fact is related to the nature of the test. ABTS radical scavenging assays evaluate molecules that have hydrophobic (methyl, aromatic groups) and hydrophilic (carboxyl, carbonyl, hydroxyl) groups, unlike the DPPH scavenging assay that evaluates more hydrophilic molecules [15,19,20,23]. The lignins under study did not present IC_{50} for the reduction assays of molybdenum and iron ions, that is, they were not able to promote the transfer of hydrogen and electrons necessary for the reduction of these ions.

The antioxidant activity promoted by lignins is directly related to their chemical structure [71,72]. The ortho-methoxy substitution found in the G, S, and H units of lignin act as antioxidants not only because of their ability to donate hydrogen or electrons but also because of their stable intermediate radicals, which prevent oxidation [15,19,23,71,72]. However, the antioxidant activity is not attributed only to the phenolic groups, the conjugated double bonds also play an important role, they promote an additional stabilization of the phenoxyl radicals through prolonged relocation, which may contribute to the increase of the activity [71,72]. It is worth noting that lignins with high contents of conjugated carbonyl groups and aliphatic hydroxyl groups promote low activities [15,23,71,72]. Therefore, understanding the structural arrangement of lignin is one of the steps for its use as an antioxidant agent [71,72].

The literature presents promising results of ABTS $^{\bullet+}$ radical scavenging activity for different alkaline lignins. Table 6 summarizes some of these results showing the type of lignin and IC_{50} values (μg/mL). These results confirm that understanding the chemical structure of lignins is an important step in their investigation as an antioxidant agent [15,19,23,71,72] [73].

3.4. Assays of cytotoxic activities in mammalian cells promoted by lignins from the branch and leaves of Buchenavia viridiflora

In vitro cytotoxicity assays enable the analysis of the toxic or antiproliferative effect of samples in cell culture [74]. Therefore, they are extremely relevant to the development of new drug candidate molecules [75]. For this study, assays were carried out with macrophage cells, whose main function is to carry out phagocytosis (acting mainly in infectious processes). Macrophages are the first line of defense against different cellular invaders that cross epithelial barriers, they can phagocytose damaged and aged cells, cellular debris, foreign agents (different microorganisms), and inert particles [74,75]. During phagocytosis, macrophages produce different concentrations of reactive oxygen and nitrogen species, mainly nitric oxide, by the action of an enzyme called nitric oxide synthase to fight the invader, however, an overproduction of nitric oxide can promote cell damage [74,75].

Therefore, the cytotoxic effect of different lignins against macrophages of the J774 A1 strain was initially analyzed using the MTT colorimetric method. In parallel to the cytotoxicity assay, the determination of nitric oxide (in the cell supernatant) was performed by the colorimetric method using the Griess reagent, to assess whether the lignins were capable of inducing an increase in the production of nitric oxide. These results were presented in Fig. 11.

The assays were carried out in J774A.1 macrophage cell revealed that the lignin obtained from the branch had an IC_{50} of 28.47 ± 0.26 μg/mL, being less toxic than the lignin from the leaves, which presented an IC_{50} of 22.58 ± 0.61 μg/mL.

IC_{50} analysis revealed that the macromolecules of this study promoted significant cytotoxic effects only at very high concentrations, as can be seen at concentrations of 25 and 100 μg/mL, where cell viability was below 40 % with a significance of $p < 0.05$. According to the results obtained in Fig. 11B, it is noted that there was an increase in nitric oxide production at concentrations of 25 and 100 μg/mL in the control and the other concentrations evaluated. Thus, the increase in nitric oxide is associated with cell damage according to the experimental conditions evaluated.

Other important cells are red blood cells, also known as red blood cells or erythrocytes, they are the cells present in the blood and are

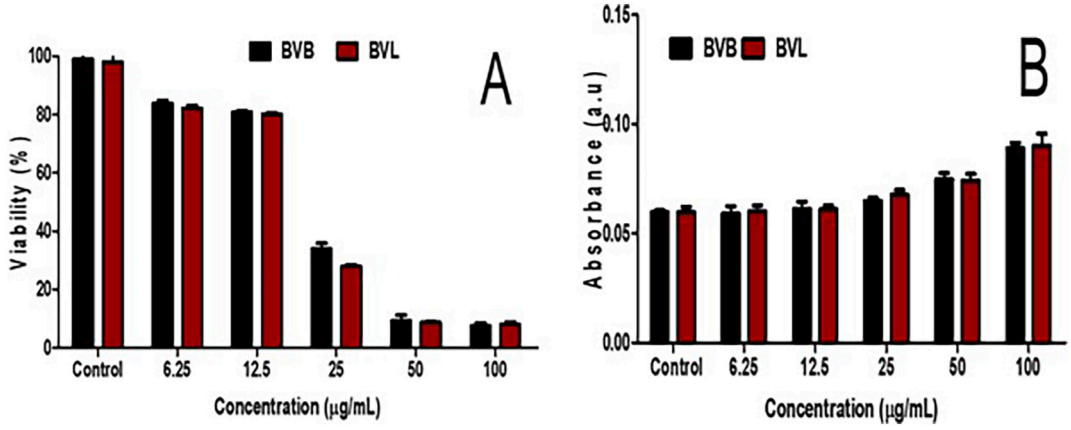

Fig. 11. Results of cell viability (A) and production of nitric oxide in cells in macrophages J774 A.1 (B) in assays performed with lignins obtained from branches (BVB) and leaves (BVL) of *Buchenavia viridiflora*.

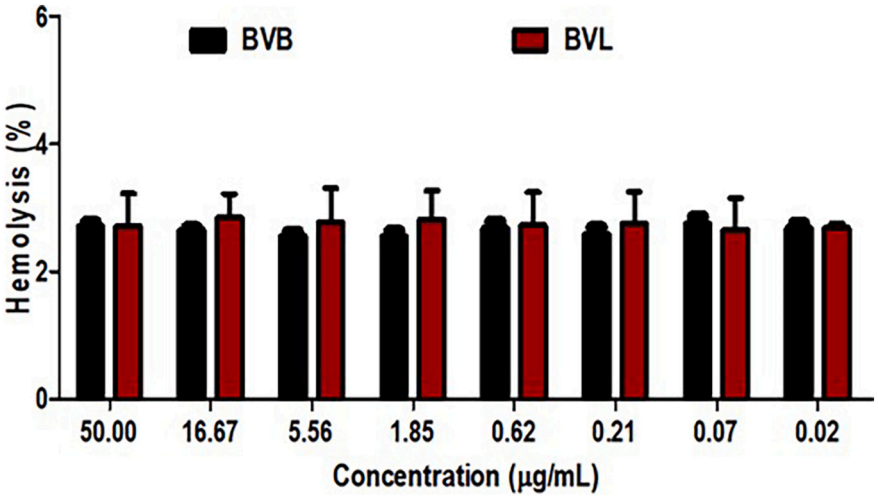

Fig. 12. Results of hemolytic activity in percentage by branch (BVB) and leaf (BVL) lignins of *Buchenavia viridiflora* compared to chloroquine and dihydroartemisinin at different concentrations.

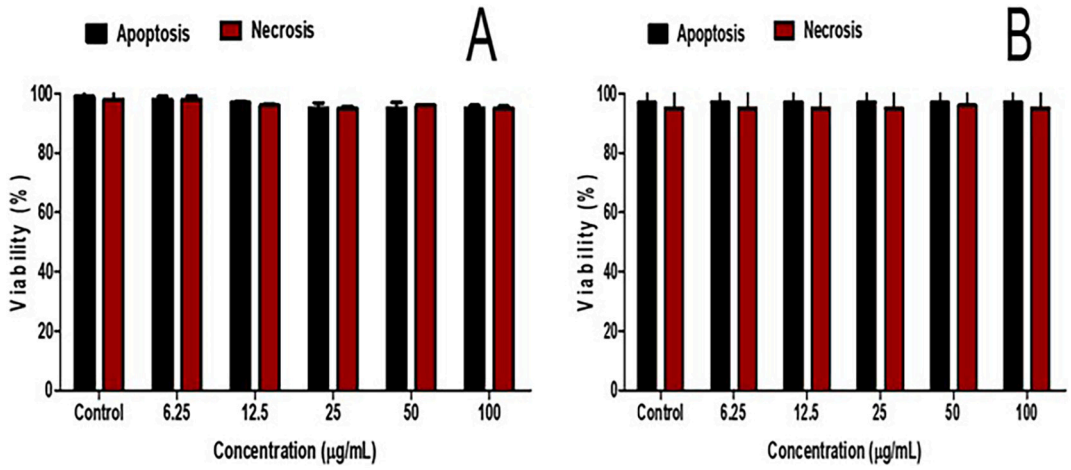

Fig. 13. Viability of mouse splenocytes promoted by lignins from branches (A) and leaves (B) of *Buchenavia viridiflora* evaluated by staining with Annexin V and Propidium Iodide in flow cytometry (FacsCalibur - BD®) at different concentrations in a 24-h period.

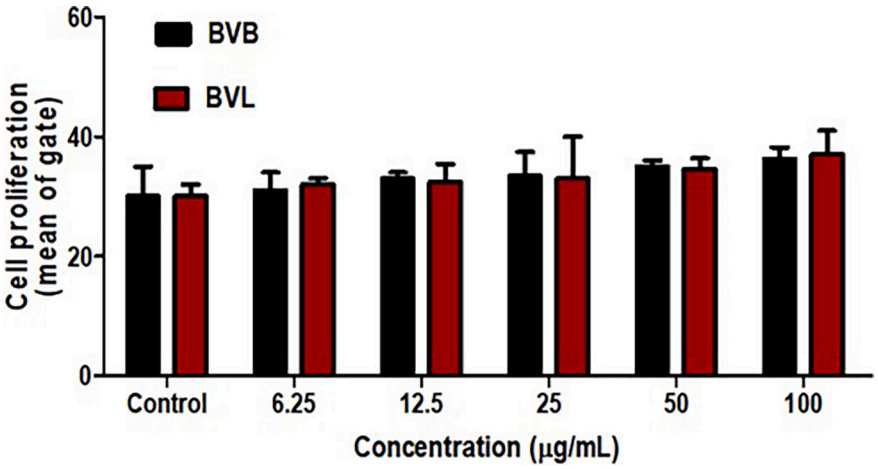

Fig. 14. Proliferation of splenocytes in mice promoted by lignins from the branches (BVB) and leaves (BVL) of *Buchenavia viridiflora* evaluated by staining with Annexin V and Propidium Iodide in flow cytometry (FacsCalibur - BD®) at different concentrations in a 24-h period.

Table 7
Production of cytokines and nitric oxide promoted in mice by lignins from branches (BVB) and leaves (BVL) of *Buchenavia viridiflora* at a concentration of 12.5 μg/mL for 24 h of splenocyte incubation.

Cytokines	Control	Lig.BVB	Lig. BVL
IL-2	8.32 ± 0.1	11.50 ± 1.0	10.1 ± 0.2
IL-4	7.34 ± 0.5	10.90 ± 0.1	9.98 ± 0.01
IL-6	10.34 ± 0.4	13.24 ± 0.8	11.39 ± 0.1
IL-10	13.21 ± 0.2	15.39 ± 0.4	14.02 ± 0.9
IL-17	5.39 ± 0.0	5.54 ± 0.1	5.42 ± 0.1
TNF-α	6.39 ± 0.1	6.41 ± 0.2	6.40 ± 0.1
IFN-γ	7.53 ± 0.1	7.55 ± 0.4	7.59 ± 0.2
Nitric oxide	Control	Lig.BVB	Lig. BVL
Concentration (μg/mL)	0.08 ± 0.0	0.12 ± 0.02	0.10 ± 0.01

Mean ± Standard Deviation.

responsible for carrying oxygen to all body tissues [76]. Toxic molecules to erythrocytes compromise the functionality of the organism [77]. Therefore, it is necessary to perform hemolytic assays to verify if the molecule promotes cellular data to these cells [76,77].

Hemolytic assays are easy to perform, low cost and have good results when it comes to cytotoxicity [76]. These assays performed with erythrocytes are mainly related to mechanisms of membrane damage in these cells [46,47]. The erythrocyte membrane is the primary model for studying animal cell plasma membranes, as it lacks a nucleus and organelles [46,76,77].

Plasma membranes, in general, present themselves as selective barriers that ensure the constant internal composition of cells, through the control of the active and passive transfer of numerous molecules [76,77]. These membranes have a complex structural system, the cytoskeleton, which involves both the shape of the cell, its mobility, deformability, and the transport of macromolecules [46,76]. Among the different constituents of the membrane, there are receptors involved in complex functions that allow communication between cells, immunological recognition, and cell adhesion phenomena [76,77]. Therefore, damage to these membranes leads to the death of the organism [46,47,76,77].

The lignins in this study were evaluated for cytotoxicity against erythrocytes. Fig. 12 shows the results in terms of the percentage of hemolysis for lignins from branches (BVB) and leaves (BVL) at different concentrations.

The lignins in this study showed hemolytic activity below 5 %. It is well known that in *in vitro* hemolysis assays, results below 10 % indicate that the molecule is non-hemolytic, while values above 25 % are considered hemolytic [76,77]. Therefore, the lignins in this study and chloroquine did not show toxicity against erythrocytes. The literature presents results of hemolytic activity for different materials containing lignin and these did not present cytotoxicity against erythrocytes.

Siddiqui et al. [78] evaluated hemolytic activity promoted by lignin nanoparticles, they found that they promoted percentages lower than 2 % at concentrations ranging from 100 to 1000 μg/mL. Other authors also obtained low results of hemolytic activity for nanoparticles composed of lignins, among which we can mention: Lee et al. [79] obtained results below 10 % at concentrations ranging from 200 to 800 μg/mL. Dai et al. [80] obtained results below 5 % at concentrations ranging from 100 to 1000 μg/mL. These results indicate that the lignins obtained in our study have low *in vitro* toxicity. Espinoza-Acosta et al. [81] their review of the literature on the biological effects of lignins, observed that the lignins evaluated were cytotoxic only at concentrations >700 μg/mL.

3.5. *In vitro immunomodulation assays*

Splenocytes were cultured with different concentrations (100 to 6.25 μg/mL) of the lignins under study, to evaluate possible cytotoxic effects. For this, propidium iodide (cell death by necrosis) and annexin V (apoptosis cell death) were used. The viability is shown in Fig. 13.

The results showed that lignins were not able to promote significant death in animal cells and can be safely used at all concentrations evaluated in this study. Similar results were obtained by Cruz-Filho et al. [22], Santos et al. [19], Melo et al. [23], and Arruda et al. [15]

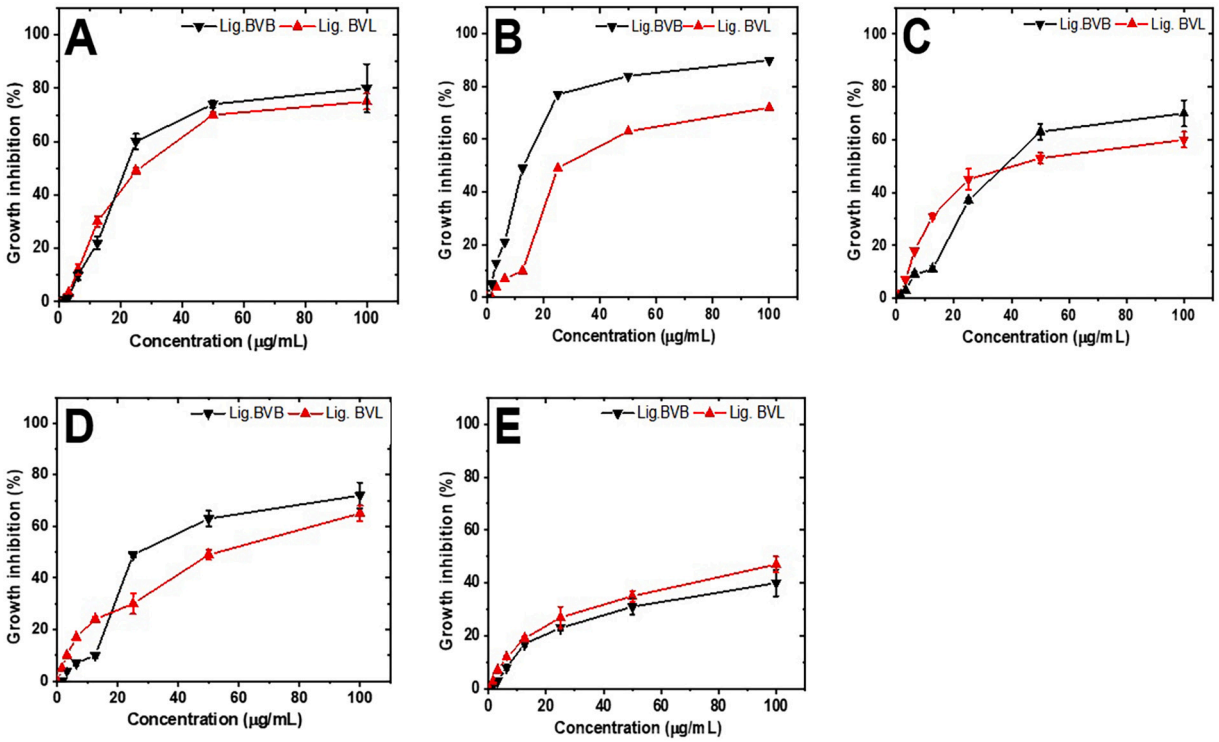

Fig. 15. Results of *in vitro* antitumor activity promoted by lignins from twigs (BVB) and leaves (BVL) of *Buchenavia viridiflora* compared to different patterns (Doxo: doxorubicin m-Amsa: amsacrine and Asul: asulacrine) against different cells of Jurkat cancer (A), MCF-7 (B), DU-145 (C), T47D (D) and HepG2 (E).

Table 8
In vitro antitumor activity assays promoted by lignins from branches (BVB) and leaves (BVL) of *Buchenavia viridiflora* compared to different patterns and results of selectivity index.

Samples	Jurkat IC_{50} (μg/mL)	IS	MCF-7 IC_{50} (μg/mL)	IS	DU145 IC_{50} (μg/mL)	IS	T47D IC_{50} (μg/mL)	IS	HepG2 IC_{50} (μg/mL)	IS
Lig. BVB	21.37 ± 0.3	1.33	12.63 ± 0.4	1.14	37.56 ± 0.3	0.80	25.46 ± 0.3	1.12	>100	<0.28
Lig. BVL	25.76 ± 0.1	0.03	24.88 ± 1.0	0.91	41.65 ± 1.1	0.54	47.74 ± 0.1	0.47	>100	<0.22
Doxo	0.7 ± 0.0	81.0	1.0 ± 0.3	56.7	0.76 ± 0.0	74.6	1.0 ± 0.3	56.7	1.54	36.8
m-Amsa	1.4 ± 0.1	68.21	1.3 ± 0.1	73.46	0.80 ± 0.01	119.37	1.2 ± 0.4	79.58	1.37	69.7
Asul	1.3 ± 0.1	84.69	1.2 ± 0.1	91.75	0.66 ± 0.0	166.81	1.2 ± 0.4	91.75	1.45	75.9

Mean ± Standard deviation; IC_{50} values for J774 macrophages: Doxo: doxorubicin (IC_{50} 56.7 μg/mL); m-Amsa: amsacrine (IC_{50} 95.5 μg/mL) and Asul: asulacrine (IC_{50} 110.1 μg/mL).

evaluating the cytotoxicity promoted by different alkaline lignins against immune cells. After verifying the high cell viability promoted by lignin, the splenocytes were submitted to three different concentrations of lignin (100 to 6.25 μg/mL), for 24 h, to evaluate cell proliferation. The results are shown in Fig. 14.

The results showed that lignins were able to induce a non-significant cell proliferation under the conditions studied. Similar results were obtained by Cruz-Filho et al. [22], Melo et al. [23], and Santos et al. [19] evaluating different alkaline lignins. Seven cytokines comprising the Th1, Th2, and Th17 profiles were investigated. For the determination of these, only the concentration of 12.5 μg/mL was used, a non-toxic concentration against the splenocytes, macrophages, and erythrocytes evaluated in this study. Table 7 presents the results of cytokine production promoted by each of the lignins in our study.

Lignins were able to significantly induce the production of most anti-inflammatory cytokines, that is, of the Th2 profile, such as the cytokines IL-4, IL-10, and IL-6, the latter being pleiotropic. The other cytokines were produced at basal values (similar to the control) and, therefore, did not promote changes in the immunological status in cultures. Furthermore, the increase in nitric oxide without promoting cell death proves that the lignins evaluated here promote an anti-inflammatory effect *in vitro*. The production of cytokines is directly related to the chemical structure of lignins, these macromolecules can interact in different ways promoting different responses.

Cruz-Filho et al. [22] found that the alkaline lignins of *Opuntia ficus-indica* and *Opuntia cochenillifera* stimulate the pro-inflammatory response through the production of the cytokines TNF-α, IL-6, and IL-10.

Melo et al. [23] found that IL-4 and IL-10 cytokines were greater than IL-2 and IFN-γ production and suggested a prevalent Th2 response. Its anti-inflammatory behavior associated with the production of TNF-α and IL-6 may induce a potential healing action by the lignin *Caesalpinia pulcherrima*.

Santos et al. [19] observed a large increase in IL-2, IL-4, IL-6, TNF-α, and IFN-γ levels, while a moderate increase in IL-10 was observed in response to stimulation of alkaline lignin from *Conocarpus erectus*. There was a greater increase in the levels of cytokines secreted by cells involved in the Th1 response, indicating a predominant pro-inflammatory response.

Arruda et al. [15] found that lignin from *Crataeva tapia* stimulated the production of TNF-α, IL-6, and IL-10, suggesting a potential role of this lignin in the inflammatory phase of wound healing. These results show that the lignins evaluated in this study can promote promising immunomodulatory activity.

3.6. *In vitro* cytotoxic activity against tumor cells

The *in vitro* cytotoxic activity of the lignins under study was determined by the MTT method, where five different cell lines were evaluated: MCF-7 (breast cancer), T-47D (breast cancer), Jurkat (leukemia/lymphoma), DU145 (human prostate cancer cell) and HepG2 (hepatoma). Fig. 15 shows the results of cell growth inhibition at different concentrations.

The curves presented in Fig. 15 show that lignins promote an increase in cellular inhibition with increasing concentration. A similar profile was found by Andrijevic et al. [82], Wang et al. [63,64] and Barapatre et al. [83] evaluating different lignins and their fractions. Table 8 presents the results of IC_{50} promoted by lignins for each of the cells and selectivity index.

The results show that lignins presented IC_{50} values (concentration that inhibits growth by 50 %) for all cells except for the HepG2 lineage. Twig lignins were able to promote higher inhibition values when compared to leave lignins. Lower IC_{50} values represent higher inhibition values, therefore, we can group the results in the following order: MCF-7 > Jurkat > T47D > DU145 > HepG2. From these results, we can highlight the results promoted by the lignin of the branches against MCF-7 and Jurkat cells, being more toxic against these cells when compared to normal cells (macrophages). Even with low levels of selectivity, it was able to promote significant activity.

Table 9
Results of *in vitro* antimicrobial activity promoted by lignins from the branches (BVB) and leaves (BVL) of *Buchenavia viridiflora.*

Microorganisms	Lignin BVB		Lignin BVL		Control - antimicrobial	
Bacteria	MIC (μg/mL)	MIC (μg/mL)	MIC (μg/mL)	MBC (μg/mL)	MIC (μg/mL)	
Enterococcus faecalis UFPEDA-69	512	>1024	>1024	>1024	Amikacin	8 (S)
Enterococcus faecalis UFPEDA-138	>1024	>1024	>1024	>1024	Amikacin	8 (S)
Staphylococcus aureus UFPEDA-709	512	>1024	>1024	>1024	Oxacillin	512 (R)
Acinetobacter baumannii UFPEDA-1024	>1024	>1024	>1024	>1024	Amp. + Sulbac.	16 (I)
Pseudomonas aeruginosa UFPEDA-261	512	>1024	>1024	>1024	Amikacin	32 (I)
Pseudomonas aeruginosa UFPEDA-416	>1024	>1024	>1024	>1024	Amikacin	8 (S)
Yeasts	MIC (μg/mL)	MIC (μg/mL)	MIC (μg/mL)	MFC (μg/mL)	MIC (μg/mL)	
Candida albicans UFPEDA-1007	>1024	>1024	>1024	>1024	Micafungin	0.0625 (S)
Candida albicans 95	>1024	>1024	>1024	>1024	Micafungin	0.0312 (S)
Candida albicans 4664	512	>1024	>1024	>1024	Micafungin	0.0156 (S)
Candida glabrata UFPEDA-6393	>1024	>1024	>1024	>1024	Micafungin	0.0156 (S)
Candida guilliermondii UFPEDA-6390	>1024	>1024	>1024	>1024	Micafungin	0.0156 (S)

Legend: MIC – Minimum inhibitory concentration; MBC – Minimum bactericidal concentration; MFC – Minimum fungicidal concentration; R - Resistant; S – Sensitive; I – Intermediate resistance; Amp. + Sulbac – Ampicillin+Sulbactam.

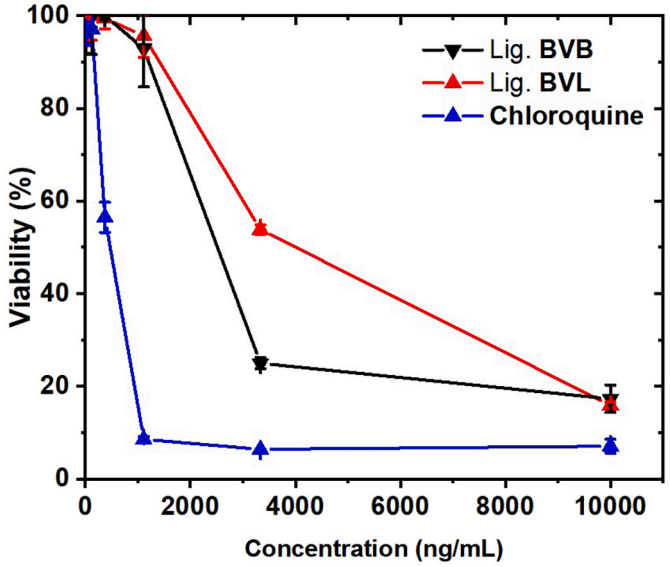

Fig. 16. Results of cytotoxicity against the chloroquine-sensitive strain of *Plasmodium falciparum* 3D7 in percentage promoted by the lignins of the branch (BVB) and leaves (BVL) of *Buchenavia viridiflora* compared to chloroquine at different concentrations.

Other authors also evaluated the antiproliferative activity promoted by different lignins and their fractions. Barapatre et al. [83] found that four lignin fractions obtained from *Acacia nilotica* wood showed higher cytotoxic potential (IC_{50}: 2–15 μg/mL) in the breast cancer cell line (MCF-7). Guo et al. [84] also obtained promising inhibition results against the MCF-7 strain. Aadil et al. [85] evaluated the *in vitro* cytotoxicity activity of lignin-mediated AGNPs (5–500 μg/mL) demonstrated toxicity effects on MCF-7 and A375 melanoma cell lines. These findings prove that lignins are capable of inhibiting the growth of tumor cells.

3.7. In vitro antimicrobial activity

The antimicrobial potential of lignins was initially evaluated by the microdilution method in 96-well plates, to determine the minimum inhibitory concentration and minimum bactericidal or fungicidal concentration. The results of antimicrobial activity were presented in Table 9.

The results presented in Table 9 showed that only the lignin of the branches was able to promote antimicrobial activity, presenting a minimum inhibitory concentration of 512 μg/mL for the bacteria *Enterococcus faecalis* UFPEDA-69, *Staphylococcus aureus* UFPEDA-709, *Pseudomonas aeruginosa* UFPEDA-261 and for the yeast *Candida albicans* 4664. In addition, none of the lignins evaluated showed minimal bactericidal or fungicidal concentration.

The antimicrobial activity promoted by lignins is directly related to the chemical structure [23,81,86]. The mechanism of antimicrobial activity promoted by lignins is not fully understood. However, according to Espinoza-Acosta et al. [81] lignins that present higher amounts of phenolic fragments containing a C—C double bond in the α and β positions of the side chain and a methyl group in the γ position promote greater inhibition of microbial growth when compared to lignins that present higher levels of phenolic fragments with functional groups containing oxygen (–OH, –CO, COOH) in the side chain.

In our study, the greater activity promoted by the lignin of the branch may have been attributed to a lower content of -OH, -CO, and -COOH groups, in addition to presenting a more condensed structure, when compared to the lignin of the leaves, which did not promote antimicrobial activity. at the concentrations evaluated.

Different studies have shown that lignin has promising antimicrobial activity. Melo et al. [23] evaluating the *in vitro* antimicrobial potential of lignin isolated from leaves of *Caesalpinia pulcherrima* found that they were able to inhibit the growth of *Candida parapsilosis* (ATC22019), *Candida krusei* (ATC62), *Candida guilliermondii* (URM62), *Candida albicans* (URM49), *Aspergillus flavus*, *Aspergillus furmigatus*, *Cryptococcus neoformans* (HC44), *Cryptococcus neoformans* (HC43) at concentrations ranging from 15.52 to 500 μg/mL.

Pletzer et al. [87], obtaining silver nanoparticles with an antimicrobial lignin coating, observed that they were able to inhibit the growth of *A. baumannii* (ATCC BAA-747), *A. baumannii* 808, *E. casseliflavus* 1, *E. coli* (ATCC 25922), *K. pneumoniae* 124, *P. aeruginosa* (ATCC 14210), *P. aeruginosa* 205, *P. aeruginosa* LESB58, *S. aureus* 700, *S. aureus* LAC and *S. aureus* MRSA (ATCC 700698) at concentrations ranging from <1.0 to 5.0 μg/mL.

Wang et al. [88] evaluating different lignin fractions observed that the F1 fraction exhibited growth inhibitory effects against two Gram-positive bacteria (*Staphylococcus aureus* and *Bacillus subtilis*) and two Gram-negative bacteria (*Escherichia coli* and *Salmonella enterica*) with MICs of 1, 2, 2 and 2 mg/mL, respectively.

These results show the potential of lignins against *Enterococcus faecalis* UFPEDA-69, *Staphylococcus aureus* UFPEDA-709, *Pseudomonas aeruginosa* UFPEDA-261 and *Candida albicans* 4664.

3.8. In vitro antiparasitic activity against strains of Plasmodium falciparum

The results of *in vitro Plasmodium falciparum* activity were divided into two moments, the first evaluating the cytotoxicity against the chloroquine-sensitive strain of *Plasmodium falciparum* 3D7. And a second moment using the chloroquine-resistant strain of *Plasmodium falciparum* (Dd2).

The cytotoxicity assays against the 3D7 strain (*Plasmodium falciparum* sensitive to chloroquine) were performed according to the results obtained in the cytotoxicity assays in macrophages and erythrocytes. Therefore, they were performed at concentrations lower than 10 μg/mL (10,000 ng/mL), and these concentrations were sufficient to promote the death of the parasite. The exposure time of the lignins and the chloroquine standard with the cells was 72 h. This time was established because it is the period necessary for the parasite to multiply (inside the cells), break the blood cells, and start a new cycle invading new cells [49,50].

Fig. 16 shows the results of toxicity promoted by lignins from the branch and leaves of *Buchenavia viridiflora* at different concentrations compared to the commercial drug chloroquine against the 3D7 strain (*Plasmodium falciparum* sensitive to chloroquine). The results were expressed as a percentage of cell viability.

The results show a decrease in viability with increasing concentration, this profile was also observed by Banzragchgarav et al. [89] and Akaddar et al. [90] evaluating the activity of different natural products against the same strain of *Plasmodium falciparum* used in this study.

Through the curves obtained, it was possible to determine the IC_{50} (concentration capable of inhibiting the growth of the parasite by 50 %) in ng/mL. The results showed that the drug chloroquine (156.83 ± 0.01 ng/mL) was more toxic when compared to lignin from branches (2511.44 ± 0.1 ng/mL) followed by lignin from leaves (4892.38 ± 0.7 ng/mL).

The mechanism of action of lignins against *Plasmodium falciparum* strains has not yet been reported in the literature, however, the use of different phenolics has already been well described [89,91,92]. The mechanisms of phenolic compounds are diverse, inhibiting important enzymes in the metabolism of the parasite, in addition, they can promote DNA denaturation and damage the plasma membrane [89,92]. However, because lignins have high structural complexity and are larger than

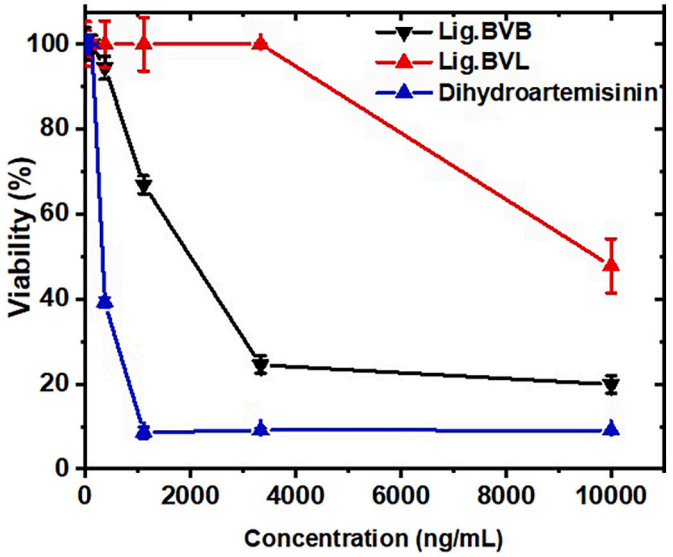

Fig. 17. Cytotoxicity results against the chloroquine-sensitive strain of *Plasmodium falciparum* (Dd2) in percentage promoted by the lignins of the branch (BVB) and leaves (BVL) of *Buchenavia viridiflora* compared to chloroquine at different concentrations.

chloroquine, they can mainly cause damage to the plasma membrane of the parasite, as they have low hemolytic activity. In addition to being of low molecular weight, they can cross the erythrocyte membrane. Similar behavior, this is, damage to the surface of the parasite, was observed by Silva et al. [20] where the authors evaluated the effects of low molecular weight alkaline lignin obtained from *Morinda citrifolia* leaves against a parasite of the genus *Leishmania*. Damage to the surface of the parasite and damage to organelles were observed. These alterations were observed by different electron microscopy.

In addition to the assays carried out with the chloroquine-sensitive strain, assays were carried out with the chloroquine-resistant strain, under the same experimental conditions of cultivation of the 3D7-GFP strain. Due to the indiscriminate use of antimalarial agents, the parasites have become resistant to the drugs available [93].

The *Plasmodium falciparum* strain (Dd2) is one of the examples of chloroquine-resistant parasites of the genus *Plasmodium*. Therefore, other drugs have been used for the treatment of this parasitosis [93,94]. Among these, we can mention dihydroartemisinin, a fast-acting multi-target drug when compared to other antimalarials [94]. This is because it inhibits the early stages of development of the *Plasmodium* parasite, as soon as it invades the erythrocytes [93,94]). Most antimalarials act on late trophozoite and schizont stages, while dihydroartemisinin acts on young trophozoites and ring stages. Due to its ring-shaped action, dihydroartemisinin prevents the development of the early sexual stage (gametocytes), resulting in reduced malaria transmission in endemic areas [94]. This drug has no action on parasites that are in the hepatic cycle [93,94].

Fig. 17 shows the results of toxicity promoted by lignins from the branch and leaves of *Buchenavia viridiflora* at different concentrations compared to the commercial drug chloroquine against the Dd2 strain (Chloroquine-resistant *Plasmodium falciparum*). The results were expressed as a percentage of cell viability.

The results show a decrease in viability with increasing concentration. A similar profile was obtained by Nugraha et al. [95] and Keumoe et al. [96] evaluating different phenolic compounds against the *Plasmodium falciparum* strain (Dd2). Through the curves obtained, it was possible to determine the IC_{50} (concentration capable of inhibiting the growth of the parasite by 50 %) in ng/mL. The results showed that the drug dihydroartemisinin (5.26 ± 0.01 ng/mL) was more toxic when compared to lignin from branches (2440 ± 0.8 ng/mL) followed by lignin from leaves (9760 ± 0.1 ng/mL). Similar behavior to that obtained for the chloroquine-sensitive strain.

Even with the scarcity of works reported on the antiplasmodium activity promoted by lignins, it is known that different lignoids, especially lignans (building blocks for the formation of lignin) can promote damage to the parasite. Among these works we can mention those proposed by Jensen et al. [97] isolating a lignan dehydrodiconiferyl dibenzoate (2) and *p*-hydroxybenzoic acid (1) were isolated from the roots of the *Euterpe precatória* palm, they found that compound 2 showed moderate antiplasmodic activity (6790 ng/mL) against the chloroquine-sensitive strain of *Plasmodium falciparum* (3D7).

Silva Filho et al. [98] isolated seven lignans (Machilin-G (1a), Galgravin (1b), Nectandrin-A (1c), Nectandrin-B (1d), Veraguensin (2a), Calopeptin (2b), from Nectandra megapotamica (Lauraceae) and Ganshisandrina (3) of *Nectandra megapotamica*. The authors observed that only calopeptin (2b) showed moderate activity, with IC_{50} values of 3800 ng/mL (*P. falciparum*, chloroquine-sensitive clone D6) and 3900 ng/mL (*P. falciparum*, clone W2 resistant to chloroquine), while lignans 1a,1b,1c 1d, 2a and 3 were inactive.

Ortet et al. [99] isolation and identification of six known furfuran lignans: eudesmin (1), magnolin (2), epimagnoline A (3), ascantine (4), kobusin (5) and sesamin (6) from *Artemisia gorgonum* obtained IC50 ranging from 3370 and 25,000 ng /mL for the *Plasmodium falciparum* strain FcB1. These results show how promising the different lignoids can be against *Plasmodium falciparum* strains.

These findings show that the lignins obtained show promising activity against different strains of *Plasmodium falciparum in vitro*.

4. Conclusion

The results of this study show that the lignins of the branches and leaves are of the GSH type, presenting higher contents of guaiacyl units, in addition to being of low molecular weight and presenting final stability. ABTS radical scavenging assays, whose lignin may have moderating power in the radical scavenging assay. Lignins showed low toxicity against different animal cells, in addition, they were able to induce the production of anti-inflammatory cytokines *in vitro*. These were also able to inhibit the growth of tumor and microbial cells and of *Plasmodium falciparum* species (the causative agent of malaria). Therefore, this information is important or potential biological products that can be applied in the pharmaceutical and biomedical areas.

Declaration of competing interest

None.

Data availability

Data will be made available on request.

Acknowledgment

The study was funded by Foundation for the State of Pernambuco (Process - FACE-04.03/19), AP Researcher Research Grant - FACEPE (Process BFP-0038-0) and National Council for Scientific and Technological Development grant - CNPq (Process 306865/2020-3). This research was also funded by the Foundation for Science and Technology (FCT) through the GHTM (UID/04413/2020). Thanks to MR4, who provided us with the *Plasmodium falciparum* strains that we used in the assays. We also thank the Laboratory of Magnetic Resonance of the Institute of Chemistry and Biotechnology (Federal University of Alagoas-UFAL) for the analysis of NMR. In addition to these, we would also like to thank Mil Madeiras Preciosas, a subsidiary of the Swiss group Precious Woods (http://preciouswoods.com.br/) for providing samples of branches and leaves of *Buchenavia viridiflora*.

References

[1] A. More, T. Elder, Z. Jiang, A review of lignin hydrogen peroxide oxidation chemistry with emphasis on aromatic aldehydes and acids, Holzforschung 75 (9) (2021) 806–823, https://doi.org/10.1515/hf-2020-0165.

[2] N.N. Solihat, F.P. Sari, F. Falah, M. Ismayati, M.A.R. Lubis, W. Fatriasari, W. Syafii, Lignin as an active biomaterial: a review, Jurnal Sylva Lestari 9 (1) (2021) 1–22, https://doi.org/10.23960/jsl191-22.

[3] J. Sternberg, O. Sequerth, S. Pilla, Green chemistry design in polymers derived from lignin: review and perspective, Prog. Polym. Sci. 113101344 (2021), https://doi.org/10.1016/j.progpolymsci.2020.101344.

[4] L. Xu, S.J. Zhang, C. Zhong, B.Z. Li, Alkali-based pretreatment-facilitated lignin valorization: a review, Ind. Eng. Chem. Res. 59 (2020) 16923–16938, https://doi.org/10.1021/acs.iecr.0c01456.

[5] H.-M. Chang, X. Jiang, Biphenyl structure and its impact on the macromolecular structure of lignin: a critical review, J. Wood Chem. Technol. 40 (2019) 81–90, https://doi.org/10.1080/02773813.2019.1697297.

[6] J. Gui, P.Y. Lam, Y. Tobimatsu, J. Sun, C. Huang, S. Cao, Y. Zhong, T. Umezawa, L. Li, Fiber-specific regulation of lignin biosynthesis improves biomass quality in Populus, New Phytol. 226 (2020) 1074–1087, https://doi.org/10.1111/nph.16411.

[7] J. Zhang, G.A. Tuskan, T.J. Tschaplinski, W. Muchero, J.G. Chen, Transcriptional and post-transcriptional regulation of lignin biosynthesis pathway genes in populus, Front. Plant Sci. 11 (2020) 652, https://doi.org/10.3389/fpls.2020.00652.

[8] E. Bernier, C. Lavigne, P.Y. Robidoux, Life cycle assessment of Kraft lignin for polymer applications, Int. J. Life Cycle Assess. 18 (2) (2013) 520–528, https://doi.org/10.1007/s11367-012-0503-y.

[9] E. Välimäki, P. Niemi, K. Haaga, A case study on the effects of lignin recovery on recovery boiler operation, in: 2010 Int. Chem. Recover. Conf. 2010, 2010, pp. 148–159.

[10] Y. Yuan, M. Guo, Do green wooden composites using lignin-based binder have environmentaly benign alternatives? A preliminary LCA case study in China, Int. J. Life Cycle Assess. 22 (2017) 1318–1326, https://doi.org/10.1007/s11367-016-1235-1.

[11] J. Zhu, C. Yan, X. Zhang, Yang, M. Jiang, X. Zhang, A sustainable platform of lignin: from bioresources to materials and their applications in rechargeable batteries and supercapacitors, Prog. Energy Combust. Sci. 76 (2020), 100788, https://doi.org/10.1016/j.pecs.2019.100788.

[12] J.F. Kadla, S. Kubo, R.A. Venditti, R.D. Gilbert, A.L. Compere, Griffith, Carbon 40 (2002) 2913–2920, https://doi.org/10.1016/S0008-6223(02)00248-8.

[13] M. Juliane Suota, D. Merediane Kochepka, M.G. Ganter Moura, C. Luiz Pirich, M. Matos, W.L. Esteves Magalhães, L. Pereira Ramos, Lignin functionalization strategies and the potential applications of its derivatives-a review, Bioresources 16 (3) (2021) 6471–6511, https://doi.org/10.15376/biores.16.3.suota.

[14] X.J. Chen, Z.H. Li, L.D. Zhang, H.R. Wang, C.Z. Qiu, X.L. Fan, S.L. Sun, Preparation of a novel lignin-based film with high solid content and its physicochemical characteristics, Ind. Crop. Prod. 164 (2021), 113396, https://doi.org/10.1016/j.indcrop.2021.113396.

[15] M.D.M. Arruda, S.D.P.L. Alves, I.J. Cruz Filho, G.F. Sousa, G.A. Souza Silva, D.K. D. Nascimento Santos, C.M.L. Melo, Characterization of a lignin from crataeva tapia leaves and potential applications in medicinal and cosmetic formulations, Int. J. Biol. Macromol. 180 (2020) 286–298. https://doi.org/10.1016/j.ijbiomac.2021.03.077.

[16] P. Jędrzejczak, M.N. Collins, T. Jesionowski, Ł. Klapiszewski, The role of lignin and lignin-based materials in sustainable construction–a comprehensive review, Int. J. Biol. Macromol. 187 (2021) 624–650, https://doi.org/10.1016/j.ijbiomac.2021.07.125.

[17] M. Culebras, G.A. Collins, A. Beaucamp, H. Geaney, M.N. Collins, Lignin/Si hybrid carbon nanofibers towards highly efficient sustainable Li-ion anode materials, Eng. Sci. 17 (2022) 195–203, https://doi.org/10.30919/es8d608.

[18] M. Culebras, G. Ren, S. O'Connell, J.J. Vilatela, M.N. Collins, Lignin doped carbon nanotube yarns for improved thermoelectric efficiency, Adv. Sustain. Syst. 4 (11) (2020) 2000147, https://doi.org/10.1002/adsu.202000147.

[19] D.K.D.N. Santos, B.R.S. Barros, L.M.S. Aguiar, I.J. Cruz Filho, V.M.B. Lorena, C.M. L. Melo, T.H. Napoleão, Immunostimulatory and antioxidant activities of a lignin isolated from Conocarpus erectus leaves, Int. J. Biol. Macromol. 150 (2020) 69–177. https://doi.org/10.1016/J.IJBIOMAC.2020.02.052.

[20] P.R. Silva, M.D.C.A. Lima, T.P. Souza, J.M. Sandes, A.D.C.A. Lima, P.J.R. Neto, I. J. Cruz Filho, Lignin from Morinda citrifolia leaves: physical and chemical characterization, in vitro evaluation of antioxidant, cytotoxic, antiparasitic and ultrastructural activities, Int. J. Biol. Macromol. 193 (2021) 1799–1812, https://doi.org/10.1016/j.ijbiomac.2021.11.013.

[21] A. Beaucamp, M. Culebras, M.N. Collins, Sustainable mesoporous carbon nanostructures derived from lignin for early detection of glucose, Green Chem. 23 (15) (2021) 5696–5705, https://doi.org/10.1039/D1GC02062E.

[22] I.J. Cruz-Filho, B.R. Silva Barros, L.M. Souza Aguiar, C.D.C. Navarro, J.S. Ruas, V. M.B. Lorena, G.J. Moraes Rocha, A.E. Vercesi, C.M.L. Melo, M.A.S. Maior, Lignins isolated from prickly pear cladodes of the species opuntia fícus-indica (Linnaeus) miller and Opuntia cochenillifera (Linnaeus) miller induce mice splenocytes activation, proliferation and cytokines production, Int. J. Biol. Macromol. 123 (2019) 1331–1339, https://doi.org/10.1016/J.IJBIOMAC.2018.09.120.

[23] C.M.L. Melo, I.J. Cruz Filho, G.F. Sousa, G.A. Souza Silva, D.K.D. Nascimento Santos, R.S. da Silva, B.R. Sousa, R.G. Lima Neto, M.C.A. Lima, G.J. Moraes Rocha, Lignin isolated from Caesalpinia pulcherrima leaves has antioxidant, antifungal and immunostimulatory activities, Int. J. Biol. Macromol. 162 (2020) 1725–1733. https://doi.org/10.1016/j.ijbiomac.2020.08.003.

[24] I. Spiridon, P. Poni, M. Chemistry, G. Ghica, V. Alley, Biological and pharmaceutical applications of lignin and its derivatives: a mini-review, Cellul. Chem. Technol. 52 (2018) 543–550, https://doi.org/10.1016/S0142-9612(03)00314-4.

[25] T. Abudula, K. Gauthaman, A. Mostafavi, A. Alshahrie, N. Salah, P. Morganti, A. Chianese, A. Tamayol, A. Memic, Sustainable drug release from polycaprolactone coated chitin-lignin gel fibrous scaffolds, Sci. Rep. 10 (2020), https://doi.org/10.1038/s41598-020-76971-w.

[26] İ. Çalgeris, E. Çakmakçı, A. Ogan, M.V. Kahraman, N. Kayaman-Apohan, Preparation and drug release properties of lignin–starch biodegradable films, Starch-Stärke 64 (5) (2012) 399–407, https://doi.org/10.1002/star.201100158.

[27] M. Culebras, A. Barrett, M. Pishnamazi, G.M. Walker, M.N. Collins, Wood-derived hydrogels as a platform for drug-release systems, ACS Sustain. Chem. Eng. 9 (6) (2021) 2515–2522, https://doi.org/10.1021/acssuschemeng.0c08022.

[28] M. Culebras, M. Pishnamazi, G.M. Walker, M.N. Collins, Facile tailoring of structures for controlled release of paracetamol from sustainable lignin derived platforms, Molecules 26 (6) (2021), 1593, https://doi.org/10.3390/molecules26061593.

[29] M. Pishnamazi, H. Hafizi, S. Shirazian, M. Culebras, G.M. Walker, M.N. Collins, Design of controlled release system for paracetamol based on modified lignin, Polymers 11 (6) (2019) 1059, https://doi.org/10.3390/polym11061059.

[30] J. Domínguez-Robles, Á. Cárcamo-Martínez, S.A. Stewart, R.F. Donnelly, E. Larrañeta, M. Borrega, Lignin for pharmaceutical and biomedical applications–could this become a reality? Sustain. Chem. Pharm. 18 (2020), 100320 https://doi.org/10.1016/j.scp.2020.100320.

[31] H. Hatakeyama, T. Hatakeyama, Lignin structure, properties, and applications, in: A. Abe, K. Dusek, S. Kobayashi (Eds.), Biopolymers: Lignin, Proteins, Bioactive Nanocomposites, Springer, Berlin Heidelberg, Berlin, Heidelberg, 2010, pp. 1–63.

[32] D. Stewart, Lignin as a base material for materials applications: chemistry, application and economics, ind cropsProd. 27 (2008) 202–207, https://doi.org/10.1016/j.indcrop.2007.07.008.

[33] S. Sugiarto, Y. Leow, C.L. Tan, G. Wang, D. Kai, How far is lignin from being a biomedical material? Bioactive Mater. 8 (2022) 71–94, https://doi.org/10.1016/j.bioactmat.2021.06.023.

[34] G. Guo, S. Li, L. Wang, S. Ren, G. Fang, Separation and characterization of lignin from bio-ethanol production residue, Bioresour. Technol. 135 (2013) 738–741, https://doi.org/10.1016/j.biortech.2012.10.041.

[35] M. Gilarranz, F. Rodriguez, M. Oliet, J. Revenga, Acid precipitation and purification of wheat straw lignin, Sep. Sci. Technol. 33 (1998) 1359–1377, https://doi.org/10.1080/01496399808544988.

[36] A.V. Faleva, A.V. Belesov, A.Y. Kozhevnikov, D.I. Falev, D.G. Chukhchin, E. V. Novozhilov, Analysis of the functional group composition of the spruce and birch phloem lignin, Int. J. Biol. Macromol. 166 (2021) 913–922, https://doi.org/10.1016/j.ijbiomac.2020.10.248.

[37] B. Ramakoti, H. Dhanagopal, K. Deepa, M. Rajesh, S. Ramaswamy, K. Tamilarasan, Solvent fractionation of organosolv lignin to improve lignin homogeneity: structural characterization, Bioresour. Technol. Rep. 7 (2019), 100293, https://doi.org/10.1016/j.biteb.2019.100293.

[38] T. Rashid, F. Sher, T. Rasheed, F. Zafar, S. Zhang, T. Murugesan, Evaluation of current and future solvents for selective lignin dissolution—a review, J. Mol. Liq. 321 (2021), 114577, https://doi.org/10.1016/j.molliq.2020.114577.

[39] R.A. Lee, C. Bédard, V. Berberi, R. Beauchet, J.M. Lavoie, UV-vis as quantification tool for solubilized lignin following a single-shot steam process, bioresourTechnol. 144 (2013) 658–663, https://doi.org/10.1016/J.BIORTECH.2013.06.045.

[40] A. Skulcova, V. Majova, M. Kohutova, M. Grosik, J. Sima, M. Jablonsky, UV/Vis spectrometry as a quantification tool for lignin solubilized in deep eutectic solvents, BioRes 12 (2017) 6713–6722.

[41] A.V. Badarinath, K.M. RAO, C.M.S. Chetty, V. Ramkanth, T.V.S. Rajan, K. Gnanaprakash, A review on in-vitro antioxidant methods: comparisons, correlations and considerations, Int. J. PharmTech Res. 2 (2) (2010) 1276–1285.

[42] H.A. Moharram, M.M. Youssef, Methods for determining the antioxidant activity: a review, Alex. J. Food Sci. Technol. 11 (1) (2014) 31–42.

[43] M.D. Alam, N.J. Bristi, M. Rafiquzzman, Review on in vivo and in vitro methods evaluation of antioxidant activity, SPJ. 21 (2013) 143–152, https://doi.org/10.1016/j.jsps.2012.05.002.

[44] R. Murugan, T. Parimelazhagan, Comparative evaluation of different extraction methods for antioxidant and anti-inflammatory properties from Osbeckia parvifolia arn. – an in vitro approach, J. King Saud Univ. Sci. 26 (2014) 267–275, https://doi.org/10.1016/J.JKSUS.2013.09.006.

[45] A. Barapatre, K.R. Aadil, B.N. Tiwary, H. Jha, In vitro antioxidant and antidiabetic activities of biomodified ligninfrom Acacia nilotica wood, Int. J. Biol. Macromol. 75 (2015) 81–89, https://doi.org/10.1016/j.ijbiomac.2015.01.012.

[46] S. Jiang, D. Kai, Q.Q. Dou, X.J. Loh, Multi-arm carriers composed of antioxidant lignin core and poly (glycidyl methacrylate-co-poly (ethylene glycol) methacrylate) derivative arms for highly efficient gene delivery, J. Mater. Chem. B 3 (34) (2015) 6897–6904, https://doi.org/10.1039/C5TB01202C.

[47] A. Mesdaghinia, Z. Pourpak, K. Naddafi, R.N. Nodehi, Z. Alizadeh, S. Rezaei, A. Mohammadi, M. Faraji, An in vitro method to evaluate hemolysis of human red blood cells (RBCs) treated by airborne particulate matter (PM10), MethodsX 6 (2019) 156–161, https://doi.org/10.1016/j.mex.2019.01.001.

[48] L.L. Nerys, I.T.T. Jacob, A.R. Silva, A.M. Oliveira, W.R.V. Rocha, D.T.M. Pereira, M. D.C.A. Lima, Photoprotective, biological activities and chemical composition of the non-toxic hydroalcoholic extract of Clarisia racemosa with cosmetic and

pharmaceutical applications, Ind Crops Prod. 180 (2022), 114762, https://doi.org/10.1016/j.indcrop.2022.114762.
[49] L. Lobo, L.I.L. Cabral, M.I. Sena, B. Guerreiro, A.S. Rodrigues, V.F. Andrade-Neto, M.L.S. Cristiano, F. Nogueira, New endoperoxides highly active in vivo and in vitro against artemisinin-resistant Plasmodium falciparum, Malar. J. 17 (2018) 145–155, https://doi.org/10.1186/s12936-018-2281-x.
[50] G.M. Teixeira, I.R. Veríssimo de Oliveira Cardoso, F. dos Santos, J.M. Amaro de Sousa, V. da Conceição, D. Gouveia de Melo Silva, R. Duarte, R. Pereira, F. Oliveira, L.C. Nogueira, F.A. Alves, A.C. Brayner, V. da Silva Santos, A.C. Rêgo Alves Pereira, Lima Leite. Dual parasiticidal activities of phthalimides: synthesis and biological profile against Trypanosoma cruzi and Plasmodium falciparum, ChemMedChem 15 (2020) 2164–2175, https://doi.org/10.1002/cmdc.202000331.
[51] D. Watkins, M. Nuruddin, M. Hosur, A. Tcherbi-Narteh, S. Jeelani, Extraction and characterization of lignin from different biomass resources, J. Mater. Res. Technol. 4 (2015) 26–32, https://doi.org/10.1016/j.jmrt.2014.10.009.
[52] N.E. El Mansouri, J. Salvadó, Analytical methods for determining functional groups in various technical lignins, Ind. Crop. Prod. 26 (2007) 116–124, https://doi.org/10.1016/j.indcrop.2007.02.006.
[53] H. Guo, B. Zhang, Z. Qi, C. Li, J. Ji, T. Dai, A. Wang, T. Zhang, Valorization of lignin to simple phenolic compounds over tungsten carbide: impact of lignin structure, ChemSusChem 10 (2017) 523–532, https://doi.org/10.1002/cssc.201601326.
[54] G.J.M. Rocha, V.M. Nascimento, V.F.N. Silva, Enzymatic bioremediation of effluent from sugarcane bagasse soda delignification process, Waste. Biomass. Valoriz. 5 (2015) 919–929, https://doi.org/10.1007/s12649-014-9316-5.
[55] D.R. Letourneau, D.A. Volmer, Mass spectrometry-based methods for the advanced characterization and structural analysis of lignin: a review, mass spectromRev (2021), https://doi.org/10.1002/mas.21716.
[56] J. Zeng, G.L. Helms, X. Gao, S. Chen, Quantification of wheat straw lignin structure by comprehensive NMR analysis, J. Agric. Food Chem. 61 (2013) 10848–10857, https://doi.org/10.1021/jf4030486.
[57] C. Zhao, J. Huang, L. Yang, F. Yue, F. Lu, Revealing structural differences between alkaline and Kraft lignins by HSQC NMR, Ind. Eng. Chem. Res. 58 (14) (2019) 5707–5714, https://doi.org/10.1021/acs.iecr.9b00499.
[58] D.R. Naron, F.X. Collard, L. Tyhoda, J.F. Gorgens, Characterisation of lignins from different sources by appropriate analytical methods: introducing thermogravimetric analysis-thermal desorption-gas chromatography–mass spectroscopy, Ind. Crop. Prod. 101 (2017) 61–74, https://doi.org/10.1016/j.indcrop.2017.02.041.
[59] L.A.Z. Torres, A.L. Woiciechowski, V.O. Andrade Tanobe, S.G. Karp, L.C.G. Lorenci, C. Faulds, C.R. Soccol, Lignin as a potential source of high-added value compounds: a review, J. Clean. Prod. 263 (2020), 121499, https://doi.org/10.1016/j.jclepro.2020.121499.
[60] M. Wadrzyk, R. Janus, M. Lewandowski, A. Magdziarz, On mechanism of lignin decomposition - investigation using microscale techniques: py-GC-MS, py-FT-IR and TGA, Renew. Energy 177 (2021) 942–952, https://doi.org/10.1016/j.renene.2021.06.006.
[61] F. Cheng, H. Bayat, U. Jena, C.E. Brewer, Impact of feedstock composition on pyrolysis of low-cost, protein- and lignin-rich biomass: a review, J. Anal. Appl. Pyrolysis 147 (2020), 104780, https://doi.org/10.1016/j.jaap.2020.104780.
[62] H. Yang, Z. Dong, B. Liu, Y. Chen, M. Gong, S. Li, H. Chen, A new insight of lignin pyrolysis mechanism based on functional group evolutions of solid char, Fuel (2020), 119719, https://doi.org/10.1016/j.fuel.2020.119719.
[63] Q. Wang, H. Mu, L. Zhang, D. Dong, W. Zhang, J. Duan, Characterization of two water-soluble lignin metabolites with antiproliferative activities from inonotus obliquus, Int. J. Biol. Macromol. 74 (2015) 507–514, https://doi.org/10.1016/j.ijbiomac.2014.12.044.
[64] W. Wang, X. Ren, J. Chang, L. Cai, S.Q. Shi, Characterization of bio-oils and bio-chars obtained from the catalytic pyrolysis of alkali lignin with metal chlorides, Fuel Process. Technol. 138 (2015) 605–611, https://doi.org/10.1016/j.fuproc.2015.06.048.
[65] A. Lourenço, J. Gominho, A.V. Marques, H. Pereira, Variation of lignin monomeric composition during Kraft pulping of Eucalyptus globulus heartwood and sapwood, J. Wood Chem. Technol. 33 (2013) 1–18, https://doi.org/10.1080/02773813.2012.703284.
[66] A.V. Marques, H. Pereira, Lignin monomeric composition of corks from barks of Betula pendula, Quercus suber and Quercus cerris determined by Py-GC-MS/FID, J. Anal. Appl. Pyrol. 100 (2013) 88–94.
[67] A. Sequeiros, J. Labidi, Characterization and determination of the S/G ratio via Py-GC/MS of agricultural and industrial residues, Ind. Crop. Prod. 97 (2017) 469–476, https://doi.org/10.1016/j.indcrop.2016.12.056.
[68] A. Tolbert, H. Akinosho, R. Khunsupat, A.K. Naskar, A.J. Ragauskas, Characterization and analysis of the molecular weight of lignin for biorefining studies, Biofuels Bioprod. Biorefin. 8 (2014) 836–856, https://doi.org/10.1002/bbb.1500.
[69] N. El Mansouri, Q. Eddine, F. Yuan, Huang, Characterization of alkaline lignins for use in phenol-formaldehyde and epoxy resins, BioResources 6 (2011) 2647–2662.
[70] J.Z. Mao, L.M. Zhang, F. Xu, Fractional and structural characterization of alkaline lignins from carexmeyeriana kunth, Cellul. Chem. Technol. 46 (3) (2012) 193–205.
[71] H. Faustino, N. Gil, C. Baptista, A.P. Duarte, Antioxidant activity of lignin phenolic compounds extracted from Kraft and sulphite black liquors, Molecules 15 (2010) 9308–9322, https://doi.org/10.3390/molecules15129308.
[72] V. Ugartondo, M. Mitjans, M.P. Vinardell, Comparative antioxidant and cytotoxic effects of lignins from different sources, Bioresour. Technol. 99 (2008) 6683, https://doi.org/10.1016/j.biortech.2007.11.038.
[73] K.R. Aadil, A. Barapatre, S. Sahu, H. Jha, B.N. Tiwary, Free radical scavenging activity and reducing power of Acacia nilotica wood lignin, Int. J. Biol. Macromol. 67 (2014) 220–227, https://doi.org/10.1016/j.ijbiomac.2014.03.040.
[74] A.L. Niles, R.A. Moravec, T.L. Riss, Update on in vitro cytotoxicity assays for drug development, Expert Opin. Drug Discovery 3 (2008) 655–669, https://doi.org/10.1517/17460441.3.6.655.
[75] W. Li, J. Zhou, Y. Xu, Study of the in vitro cytotoxicity testing of medical devices (review), Biomed. Rep. 617–620 (2015), https://doi.org/10.3892/br.2015.481.
[76] G. Kumar, L. Karthik, K.V.B. Rao, Hemolytic activity of indian medicinal plants towards human erythrocytes: an in vitro study elixir, Appl. Bot. 40 (2011) 5534–5537.
[77] G. Jeswani, A. Alexander, S. Saraf, S. Saraf, A.Ajazuddin Qureshi, Recent approaches for reducing hemolytic activity of chemotherapeutic agents, J. Control. Release 211 (2015) 10–21, https://doi.org/10.1016/j.jconrel.2015.06.001.
[78] L. Siddiqui, J. Bag, D. Seetha, A. Mittal, H. Leekha, M. Mishra, A.K. Mishra, P. K. Verma, A. Mishra, Z. Ekielski, S.Talegaonkar Iqbal, Assessing the potential of lignin nanoparticles as drug carrier: synthesis, cytotoxicity and genotoxicity studies, Int. J. Biol. Macromol. 152 (2020) 786–802, https://doi.org/10.1016/j.ijbiomac.2020.02.311.
[79] J.H. Lee, K. Kim, X. Jin, T.M. Kim, I.G. Choi, J.W. Choi, Formation of pure nanoparticles with solvent-fractionated lignin polymers and evaluation of their biocompatibility, Int. J. Biol. Macromol. 183 (2021) 660–667, https://doi.org/10.1016/j.ijbiomac.2021.04.149.
[80] L. Dai, R. Liu, L.Q. Hu, Z.F. Zou, C.L. Si, Lignin nanoparticle as a novel green carrier for the efficient delivery of resveratrol, ACS Sustain. Chem. Eng. 5 (9) (2017) 8241–8249, https://doi.org/10.1021/acssuschemeng.7b01903.
[81] J.L. Espinoza-Acosta, P.I. Torres-Chávez, B. Ramírez-Wong, C.M. López-Saiz, B. Montaño-Leyva, Antioxidant, antimicrobial, and antimutagenic properties of technical lignins and their applications, Bioresources 11 (2016) 5452–5481.
[82] L. Andrijevic, K. Radotic, J. Bogdanovic, D. Mutavdzic, G. Bogdanovic, Antiproliferative effect of synthetic lignin against human breast cancer and normal fetal lung cell lines. Potency of low molecular weight fractions, J. BUON 13 (2008) 241–244.
[83] A. Barapatre, A.S. Meena, S. Mekala, A. Das, H. Jha, In vitro evaluation of antioxidant and cytotoxic activities of lignin fractions extracted from Acacia nilotica, Int. J. Biol. Macromol. 86 (2016) 443–453, https://doi.org/10.1016/j.ijbiomac.2016.01.109.
[84] M. Guo, T. Jin, N.P. Nghiem, X. Fan, P.X. Qi, C.H. Jang, C. Wu, Assessment of antioxidant and antimicrobial properties of lignin from corn stover residue pretreated with low-moisture anhydrous ammonia and enzymatic hydrolysis process, Appl. Biochem. Biotechnol. 184 (1) (2018) 350–365, https://doi.org/10.1007/s12010-017-2550-0.
[85] K.R. Aadil, A. Barapatre, A.S. Meena, H. Jha, Hydrogen peroxide sensing and cytotoxicity activity of acacia lignin stabilized silver nanoparticles, Int. J. Biol. Macromol. 82 (2016) 39–47, https://doi.org/10.1016/j.ijbiomac.2015.09.072.
[86] I. Ullah, Z. Chen, Y. Xiea, S.S. Khan, S. Singh, C. Yu, G. Cheng, Recent advances in biological activities of lignin and emerging biomedical applications: a short review, Int. J. Biol. Macromol. 208 (2022) 819–832, https://doi.org/10.1016/j.ijbiomac.2022.03.182.
[87] D. Pletzer, J. Asnis, Y.N. Slavin, R.E. Hancock, H. Bach, K. Saatchi, U.O. Häfeli, Rapid microwave-based method for the preparation of antimicrobial lignin-capped silver nanoparticles active against multidrug-resistant bacteria, Int. J. Pharm. 596 (2021), 120299, https://doi.org/10.1016/j.ijpharm.2021.120299.
[88] G. Wang, Y. Xia, B. Liang, W. Sui, C. Si, Successive ethanol–water fractionation of enzymatic hydrolysis lignin to concentrate its antimicrobial activity, J. Chem. Technol. Biotechnol. 93 (10) (2018) 2977–2987, https://doi.org/10.1002/jctb.5656.
[89] O. Banzragchgarav, J. Batkhuu, P. Myagmarsuren, B. Battsetseg, B. Battur, Y. Nishikawa, In vitro potently active anti-plasmodium and anti-toxoplasma mongolian plant extracts, Acta Parasitol. 1 (2021), https://doi.org/10.1007/s11686-021-00401-8.
[90] C.Doderer Akaddar, MR.Marzahn Lang, F. Delalande, M. Mousli, K. Helle, A. Van, D.Aunis Dorsselaer, B.M. Dunn, M.H. Metz-Boutigue, E. Candolfi, Catestatin, An endogenous chromogranin A-derived peptide, inhibits in vitro growth of plasmodium falciparum, Cell Mol. Life Sci. 67 (6) (2009) 1005–1015, https://doi.org/10.1007/s00018-009-0235-8.
[91] L. Mamede, A. Ledoux, O. Jansen, M. Frédérich, Natural phenolic compounds and derivatives as potential antimalarial agents, Planta Med. 86 (2020) 585–618, https://doi.org/10.1055/a-1148-9000.
[92] B. Pagmadulam, D. Tserendulam, T. Rentsenkhand, M. Igarashi, C.I. Nihei, Isolation and characterization of antiprotozoal compound-producing Streptomyces species from Mongolian soils, Parasitol Int. 74 (2020), 101961, https://doi.org/10.1016/j.parint.2019.101961.
[93] K. Patel, K.T. Batty, B.R. Moore, P.L. Gibbons, J.B. Bulitta, C.M. Kirkpatrick, Mechanism-based model of parasite growth and dihydroartemisinin pharmacodynamics in murine malaria, Antimicrob. Agents Chemother. 57 (2013) 508–516, https://doi.org/10.1128/AAC.01463-12.
[94] L.E. Heller, E. Goggins, P.D. Roepe, Dihydroartemisinin – ferriprotoporphyrin IX adduct abundance in Plasmodium falciparum malarial parasites and relationship to emerging artemisinin resistance, Biochemistry 57 (2018) 6935–6945, https://doi.org/10.1021/acs.biochem.8b00960.
[95] A.S. Nugraha, Y.D. Purnomo, A.N. Widhi Pratama, B. Triatmoko, R. Hendra, H. Wongso, P.A. Keller, Nat. Prod. Commun. 17 (1) (2022), 1934578X211068926, https://doi.org/10.1177/1934578X211068926.
[96] R. Keumoe, J.G. Koffi, D. Dize, et al., Identification of 3,3′-O-dimethylellagic acid and apigenin as the main antiplasmodial constituents of endodesmia

calophylloides benth and hymenostegia afzelii (Oliver.) harms, BMC Complement Med Ther 21 (2021) 180, https://doi.org/10.1186/s12906-021-03352-9.
[97] X. Jensen, K.M. Wu, J. Patterson, S.G. Barnes, L. Carter, In vitro and in vivo antioxidant and anti-inflammatory capacities of an antioxidant-rich fruit and berry juice blend. Results of a pilot and randomized, double-blinded, placebo-controlled, crossover study, J. Agric. Food Chem. 56 (18) (2008) 8326–8333, https://doi.org/10.1021/jf8016157.
[98] A.A. Silva Filho, E.S. Costa, W.R. Cunha, ML, A. Silva, N.P.D. Nanayakkara, J. K. Bastos, In vitro antileishmanial and antimalarial activities of tetrahydrofuran lignans isolated from Nectandra megapotamica (Lauraceae), Phytotherapy Research 22 (10) (2008) 1307–1310, https://doi.org/10.1002/ptr.2486.
[99] R. Ortet, S. Prado, E.L. Regalado, F.A. Valeriote, J. Media, J. Mendiola, O.P. Thoms, Furfuran lignans and a flavone from Artemisia gorgonum Webb and their in vitro activity against plasmodium falciparum, J. Ethnopharmacol. 138 (2011) 637–640, https://doi.org/10.1016/j.jep.2011.09.039.